This is to certify that the
thesis entitled

FABRICATION OF SUBMICROMETER-SIZED ELECTRICAL PROBES FROM GLASS-METAL COMPOSITE USING A LASER-BASED MICROPIPETTE PULLER

presented by

Nickolas M. Meyer

has been accepted towards fulfillment
of the requirements for the

Master of Science degree in Materials Science and Engineering

Major Professor's Signature

12/08/03

Date

DATE DUE	DATE DUE	DATE DUE

FABRICATION OF SUBMICROMETER-SIZED ELECTRICAL PROBES FROM GLASS-METAL COMPOSITE USING A LASER-BASED MICROPIPETTE PULLER

By

Nickolas M. Meyer

A THESIS

Submitted to
Michigan State University
in partial fulfillment of the requirements
for the degree of

MASTER OF SCIENCE

Department of Chemical Engineering and Materials Science

2003

ABSTRACT

FABRICATION OF SUBMICROMETER-SIZED ELECTRICAL PROBES FROM GLASS-METAL COMPOSITE USING A LASER-BASED MICROPIPETTE PULLER

By

Nickolas M. Meyer

Submicron electrical probes were fabricated from glass capillary tubes and thin metal wires. These probes have applications in measuring the electrical properties of materials. The probes were fabricated in a CO_2 laser based micropipette puller. Empty silica tubes have been pulled to outer diameters of less than 100 nm (outer diameter) and wire-filled glass tubes have been pulled to less than 500 nm (outer diameter). The glass absorbs the laser energy and heat is transferred to the metal wire. When both the glass and metal had softened sufficiently, the clamps at each end of the tube apply tensile force. This process draws the glass and metal down together, and results in two tapered micropipettes with a core of metal inside. The metal acts as an electrically conductive channel, which is insulated by the surrounding glass. After the fabrication method of the microprobes was established, the probes were integrated into a modified four-point probe measurement system. In this system, the microprobe is mounted onto a translation stage, and is scanned across the surface of the material, while the other three probes remain static. This allows for measurement of the electrical conductance of the sample and the contact resistance between the sample and the current leads. The fabrication issues of these probes and their applications are presented.

Dedicated to Marten and Sophia Meyer,

my loving parents.

ACKNOWLEDEMENTS

I would like to take this opportunity to extend my most humble gratitude to all those who supported me throughout my graduate studies. First and foremost I'd like to thank my advisor, Dr. Tim Hogan, without whom this opportunity would not have been possible. I can't give thanks enough for the dedication of your time, sharing of knowledge, and sound advice that I received from you.

I'd like to thank my fellow team members that assisted me along the way. Thank you from the bottom of my heart to Dr. Sim Loo, Dr. Fu Guo, Dr. Hyun Park, Chun-I Wu, Jarrod Short, Adam Downey, Luke Niewiadomski, Dr. Roger Booth, Arjun Jayaraman, and Akiko Kubota for all of the help you gave me. Your support and friendship truly made this all a positive experience. I'd also like to give thanks Dr. Jun Nogami and Dr. K. N. Subramanian for serving on my thesis defense committee.

I would like to especially acknowledge the love and support of my parents, Marten and Sophia Meyer, and my brothers, Tony and Alex. You are the reason that I made it this far. Thank you for everything you've given me and for being the wonderful people that you are. Thank you for your prayers and for your guidance. I could never repay the debt that I owe you.

I would also like to thank a very special person in my life, Andrea Baird. Thank you for your tireless support of me and for being there whenever I needed you. You helped me more than you'll ever know.

Finally, I'd like to thank almighty God for guiding my path and keeping my loved ones in his hands.

TABLE OF CONTENTS

LIST OF TABLES

LIST OF FIGURES

1. INTRODUCTION

1.1 Research Objective

The purpose of this research was to fabricate electrical probes of micron and below sized tip diameters from glass capillary tubing and metal wire with a laser-based micropipette puller. The microprobes are a glass micropipette with an electrically conducting metallic core, which is continuous to the very tip. The glass capillary tube is drawn down with a thin metal wire inside. The amount of tapering that will occur is dependant on the dimensions of the glass and metal, and the parameters programmed into the micropipette puller.

The Sutter P-2000 micropipette puller was selected for this project, mostly because of its ability to pull silica. The P-2000 employs a CO_2 laser, which heats a glass tube in the middle and then pulls it apart into two micropipettes. This puller uses five different parameters to pull micropipettes including: power of the laser, scanning length of the laser, the level of viscosity of the glass, the pull force, and the time between laser deactivation and pull initiation. These parameters are varied until a combination is discovered that will taper the glass and the metal in a uniform fashion down into small, sharp tips.

The probes were then integrated into a measurement system to explore the electrical conductivity of different samples. A variation on the four-point probe configuration was developed for these probes, which will be discussed in later sections.

The micro probe fabrication procedure and results will be presented throughout the course of this thesis; along with electrical conductivity data measured using the probes.

1.1.1 History of Probe Fabrication

In 1953, researchers at Johns Hopkins University described creating a new "low-impedance-microelectrode" to replace glass micro capillaries filled with conducting electrolyte solution [1]. These electrolyte filled micropipettes had low signal-to-noise ratio if their tips were large and had large impedance if the tips were small. Therefore, they set out to produce a metal-filled micropipette that would have a small tip and low impedance.

They describe the fabrication of a metal-filled microelectrode by melting an alloy of 50% indium and 50% tin on a hot plate. The melted metal alloy was then sucked up into a Pyrex capillary tube about halfway up the length and allowed to solidify. Then, using a micropipette puller, a tip was drawn just past the point of the solidified metal. After the tip was drawn, the micropipette was placed back onto a hot plate for a time until the solidified alloy inside melted again. An ordinary sewing pin was then inserted into the open end of the micropipette and pushed the metal to the tip [1]. This pin was then used as electrical contact. This was an early method of producing a microelectrode.

In one of the earliest publications found where the metal wire and glass capillary tube were pulled together, Bradford et al. discussed the importance of the ductility of the metal wire [2]. In their experiment, they utilized a 75 μm diameter platinum wire along with a borosilicate glass tube. They claimed that the success of the electrode fabrication was dependent on the fact that the platinum wire they were using was annealed and not hard tempered. The increased ductility of the platinum wire enabled it to be drawn down to extremely small dimensions.

Hard drawn Pt wire was tested, but they reported that this wire would not reduce in diameter during the pulling procedure. They also mention that gold wire would be a satisfactory core material though did not investigate it extensively. The ease and quickness of fabrication, small tip dimensions, and reproducibility of the electrodes (about 42% reproducibility) were three advantages of this procedure over the procedure developed by the team at Johns Hopkins.

Nanonics Imaging Ltd. reported creating micro and nanoprobes from these same group metals [3]. The process used by this company is of course proprietary, but in an article out of *Review of Scientific Instruments* by a group from the Hebrew University, they shed some light on how to create these micropipettes with a core of metal. They treated the glass-metal combination as a composite material, with the glass acting as the matrix and the metal wire acting as the reinforcement fiber.

This metal wire acts as an electrically conductive channel that is accessible from the open end of the pipette and is continuous to the tip. Thus electrical contact can be made in extremely localized areas where a vast number of applications lie in the field of material investigation and property measurement. Some examples of more current applications of microprobes will be presented in the next section.

1.2 Survey of Submicron Probe Applications

As interest continues to grow in research of physical process on microscopic and smaller levels, microprobes will become of greater and greater importance. This section will offer some examples of how these types of instruments are being used in different

research situations. A brief synopsis of four different applications utilizing microprobes or micropipette-based instruments will be presented.

1.2.1. Imaging P-N junctions by Scanning Near-field Optical Microscopy (SNOM)

One of the goals of this research project was to obtain the capability of taking measurements in extremely localized areas using fabricated microprobes. An article by G. Tallaria [4] working with Nanonics Imaging Ltd. discusses the characterization of p-n junctions based on scanning probe microscopy and conductive microprobes. The measurements presented in this article are compared to a previous study that characterized p-n junctions using Electric Force Microscopy (EFM) [4].

The properties sought out in this study were local capacitance characteristics, small-scale variations of dielectric constant and resistivity, p-n junction delineation, and oxide quality. To obtain these measurements, a scanning probe system was utilized which can collect electrical data as well as capture the topographical features of the surface of the sample. However, some difficulties arose due to uncertainty of the tip shape of the scanning probe, interaction between the tip and the contact area of the sample, and any other forces that may be present.

The samples used in this experiment were cut and lapped so that the p-n junction could easily be accessed. The oxide layer had the configuration depicted in Figure 1.1. The measurements were carried out using a Nanonics SNOM/AFM 100, which is a tapered optical fiber that is covered by a layer of gold. The tip of the fiber is curved downward in order to correctly serve as an AFM tip. The SNOM/AFM 100 is mounted on the stage of an optical microscope and connected to an AFM/STM control system.

The SNOM signal is obtained in illumination mode in near-field by sending an Ar^+ laser down through the fiber and collecting the reflected signal in far-field with a

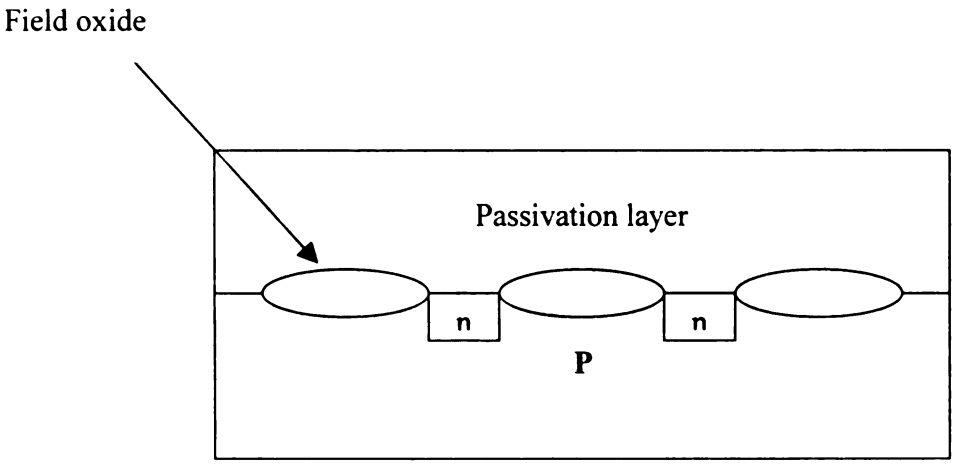

Figure 1.1 Schematic of the cross-section of the sample [4].

photo-diode. The probe is also kept in constant contact with the sample by laser feedback, which acts on the topography of the sample. For the electrical contrast of the sample, an oscillating voltage was applied to the circuit that was completed by the contact between the probe and sample. The signal was collected with a lock-in amplifier.

The result of the experiment gave the topography, the optical, and the electrical constant image all simultaneously. The parameters used in the experiment were:

- Scan area – 8 x 8 μm^2
- V_{pn} – 5V
- V_{osc} – 50 mV
- ω_{Vosc} – 100 kHz

where V_{pn} was the bias voltage, and V_{osc} was the oscillating voltage applied to the tip of the probe.

It was found that the surface of the sample was flat, topographically. There was a difference in color between the silicon and the passivation layer, and the junction was clearly seen in all three images. The electrical contrast area gives the clearest image because the depletion region acts as a capacitive area. Because an alternating current is used, the capacitive area induces the enhancement of signal in this area.

1.2.2 Measurements of MEMS in Microprobe Station

The ability to take measurements on microelectromechanical systems (MEMS) is integral to being able to predict their reliability in a service environment. An article out of the Southwest Research Institute in San Antonio, Texas uses a micro probe station to test and measure how MEMS will hold up to the vacuum of space [5]. MEMS provide advantages as space sensors and are coveted because of their small mass and size, low power requirements, and precise dimension control.

Some of the applications for the MEMS will allow them to be shielded from the space environment, such as magnetometers and gravity gradient monitors. For applications where the device is exposed to vacuum, special issues arise. Service temperature can vary by 70° C, there is high radiation exposure, and even more of a concern is vacuum welding between moving parts [5]. Because of these issues, high cycle testing of MEMS under vacuum is necessary, and requires microprobes to carry out the measurements.

The measurement system employed by this research group is similar to the one shown in Figure 1.2. This system pumps to vacuum with an ion pump, to avoid mechanical vibration, and an oil-free molecular drag pump [5]. There are four probes

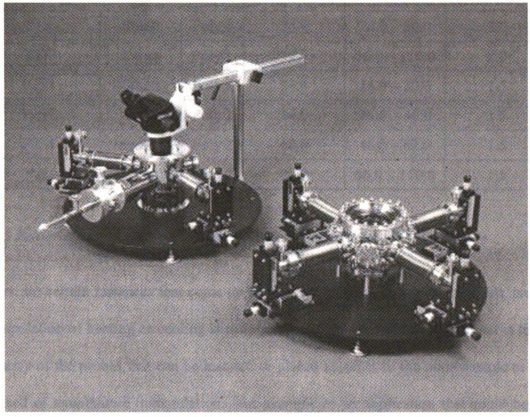

Figure 1.2 Micro probe station used in space application measurements [6].

which can be translated in the x,y, and z directions with a resolution of less than 1 μm. This control allows for manual actuation of the MEMS by using the microprobes to supply voltage to the various pads on the devices [5]. The sizes of several of the devices measured in the microprobing station are listed in Table 1.1. Some of these devices are only 26 μm in width. This requires probes with extremely fine tapers to carry out the measurement of the devices. The properties measured of the devices were such things as required operating voltage and Q – factor, or resonant frequency.

Table 1.1 Dimensions of the MEMS devices measured in micro probe station [5].

			End Mass Size (μm)		
Device Type	Size	Layer	Length (μm)	Width (μm)	Thickness (μm)
P1S	Small	Poly 1	34.0	26.0 – 30.0	2.0
P1L	Large	Poly 1	98.0	66.0 – 110.0	2.0
P2S1	Small	Poly 2	34.0	26.0 – 30.0	1.5
P2S2	Small	Poly 2	34.0	26.0 – 30.0	1.5
P2M	Medium	Poly 2	58.0	46.0 – 62.0	1.5
P2L	Large	Poly 2	98.0	66.0 – 110.0	1.5

1.2.3 Peltier-effect Module for Highly Localized Temperature Manipulations

There are certain instances that come up in biomedical research where localized, precise manipulation of heating or cooling is necessary. An answer to this requirement is to use an array of the probes that can be inserted or placed adjacent to the microsample or area in need of temperature manipulation. An example of an application that could benefit from this type of accurate heating/cooling control is in the field of metabolic research. The transmission activity of a nerve can be slowed down or even stopped when in the presence of a temperature drop, from 37° C to 5° C [7].

A restriction to this type of research is the availability of probes small enough to perform these types of localized temperature manipulation. This research done at Louisiana State University proposes constructing a device that can locally cool nerve cells in laboratory rats on a microfabricated probe [7].

The field of cryobiology could also potentially benefit from cooling devices assembled on microprobes. Cryomicroscopy is a technique used to monitor the response of cells and cellular systems to freezing temperatures. In this technique, volumes of 4 μl of cellular solution are normally used.

A problem that can arise conducting this research is that ice can form inside the cells, rupturing the membranes. If the cooling can be precisely controlled, this intracellular ice formation can be avoided [7]. A cooling microprobe can be used as a seeding probe to ensure extracellular ice formation without intracellular ice formation.

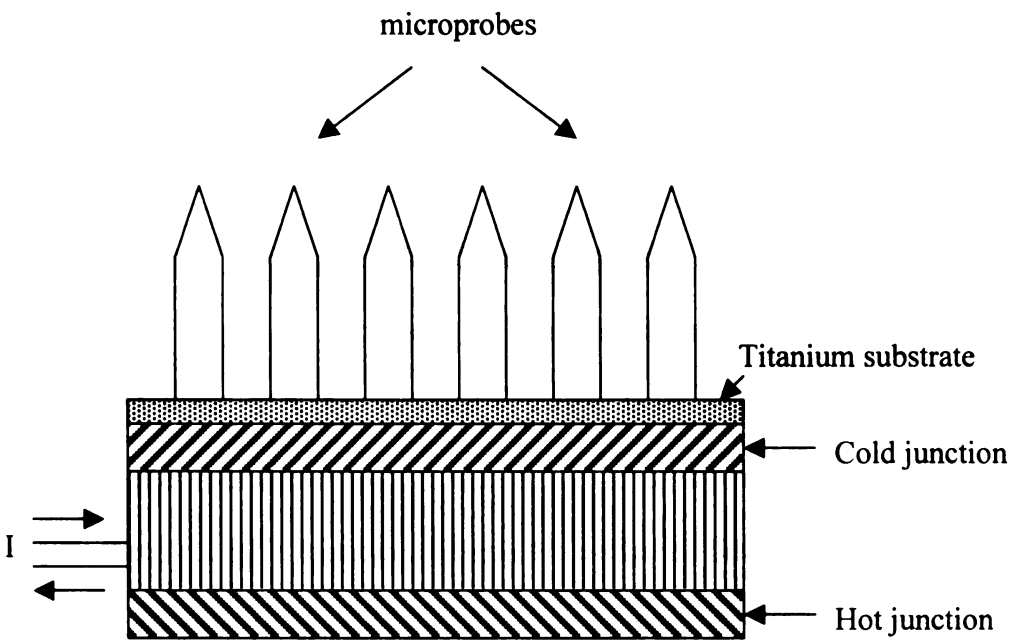

Figure 1.3 Cooling device schematic with thermoelectric chip and metallic microprobes [7].

The thermoelectric effect is taken advantage of as the driving force for the localized cooling. The cooling device is made up of two components: a cooling

thermoelectric chip and an array of metallic heat conducting microprobes attached to the top surface of the chip.

A schematic of the device is shown in Figure 1.3. The thermoelectric chip serves as the substrate, thus when an electrical current is applied, the top surface is cooled, which will be conducted through the microprobes. The current could also be reversed, and the top surface would be heated.

The microprobe array was fabricated using a technique known as the LIGA process (a graphical outline of this technique is depicted in Figure 1.4), which involves a combination of deep-etch x-ray lithography, electrodeposition, and molding to fabricate high aspect ration microstructures [7]. The LIGA process is advantageous compared to other microfabrication techniques because the ability to make microprobes from various metals and alloys.

A thin layer of polymethylmethacrylate (PMMA) is glued onto a plate of titanium. Then a mask with the design for the microstructure patterned on it is placed over the PMMA layer. It is then exposed to x-rays, leaving only the masked pattern on the metal film after the exposed portion is dissolved away in a molecular-weight sensitive solvent [7]. Then nickel is electroplated into the voids left from the x-ray lithographical process.

What is left after this step is freestanding nickel structures approximately 1000 μm in height. Then the titanium plate, with the microprobes, is attached to the thermoelectric chip via a high temperature and thermally conductive epoxy. The microprobes, made of nickel, are then coated with a biocompatible metal such as gold or platinum.

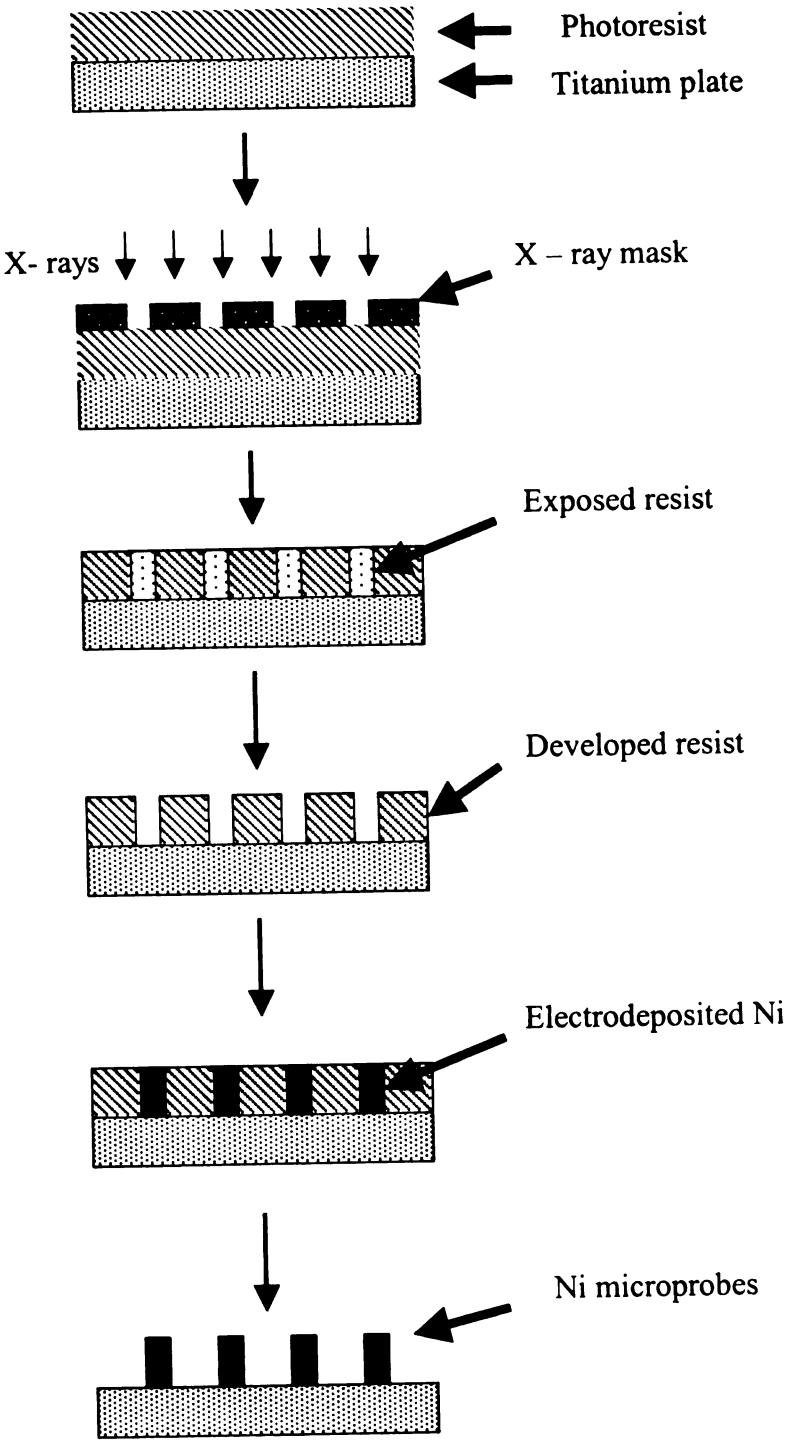

Figure 1.4 Schematic diagram of the LIGA technique [7].

1.2.4 Scanning Nanolithography Using a Material Filled Nanopipette

Hong, et al, describes a procedure that utilizes nanopipettes to deposit photoresist onto a glass substrate [8]. Conventional photolithography is extremely useful, but as electronics become smaller, more precise methods to deposit photoresist must be developed, to make way for nanolithographic techniques. The greatest limiting factor in is the ability to create a mask with micrometer and even nanometer resolution. With current technology, this is an extremely difficult task.

Using a pulled nanopipette, in combination with scanning probe microscopy such as scanning tunneling microscopy, atomic force microscopy, or near-field optical microscopy, the liquid photoresist can be deposited on the surface of the substrate through a nanometer-sized aperture.

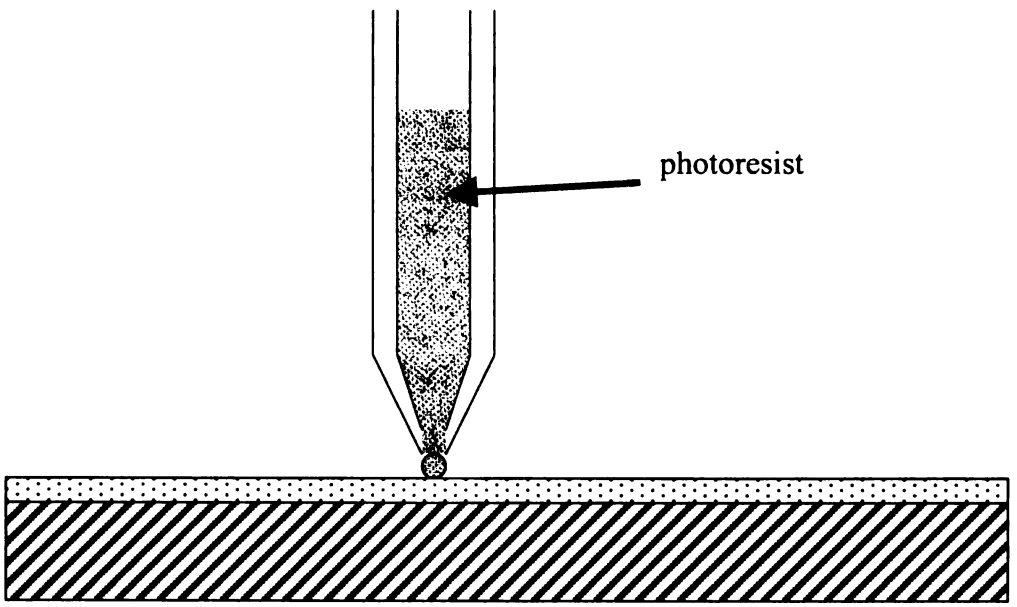

Figure 1.5 Nanopipette depositing a dot of photoresist onto a gold-coated glass substrate [8].

Liquid photoresist is deposited through the opening at the tapered tip of a quartz micropipette where the mask is basically written on the substrate. The photoresist can be deposited point-by-point, as depicted in Figure 1.5, or can be written on like a pen on paper. The micropipettes have an inner aperture at the opening of the tapered end ranging from 10 – 100 nm. With this resolution and accuracy, the designs of photoresist that could be created could be limitless.

This method eliminates the need for a mask, needs no spin on coating of photoresist, and requires no ultraviolet light source that conventional photoresist procedures use. The system developed for depositing the photoresist using the nanopipette requires that the pipette-substrate separation distance remain only a few nanometers apart. A shear force control method can be employed to regulate this particular parameter.

Dots of photoresist 300 nm in diameter were deposited on a gold-coated glass substrate at a distance of 1 μm apart. Typically, each dot was approximately 80 nm in height.

2. THEORY

2.1 Composite Material Mechanics

The glass capillary tube and metal wire, once the glass is pulled down (Fig. 2.1), can be dealt with like a glass matrix-metal fiber composite. This is the approach taken in previous studies where probes were fabricated with a micropipette puller resulting in extremely small tip diameters [9,10]. A good mechanical bond between the glass and

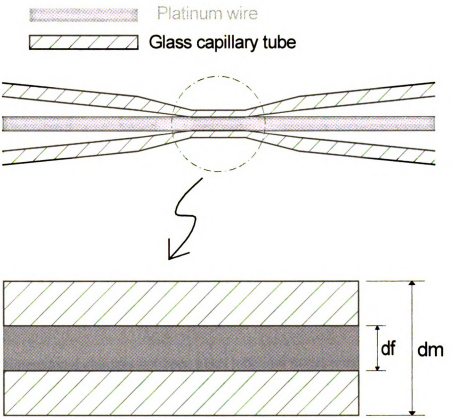

Figure 2.1 Schematic of area of glass tube of diameter, d_m, pulled down around the metal wire of diameter d_f. This is the area where the glass and metal are considered act as a composite material mechanically [10].

metal is essential, as the glass will be the only force pulling on the metal wire. Figure 2.1 is a close up schematic of the middle region of where the glass and metal wire touch for the example of platinum wire inside a glass tube. Figure 2.2 shows the dimensional changes of the glass matrix after the initial step is executed from a cross-sectional viewpoint. The inner and outer diameters deform concentrically, and the thickness of the tube remains constant.

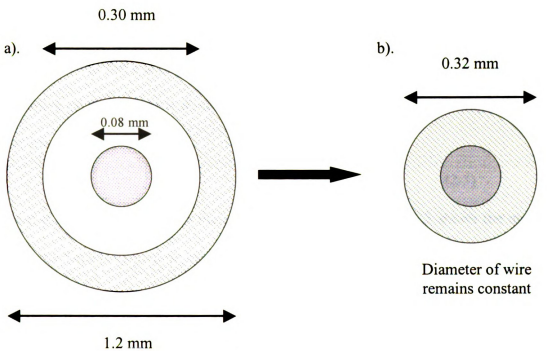

Figure 2.2 Dimensional changes between glass tube and metal wire a). before the initial pull and b). after the initial pulling step (not to scale). This is a cross-sectional view of Fig. 2.1.

Assuming that there is good bonding between the glass and metal then some aspects of the mechanical behavior of the system can be assumed. Namely, the glass and metal should deform in the same manner under the right conditions (dimensions,

micropipette puller parameters, etc). Therefore, each component should experience the same amount of strain, ε (change in length/original length),

$$\varepsilon = \varepsilon_c = \varepsilon_m = \varepsilon_f, \qquad (2.1)$$

where ε_c is the strain on the composite, ε_m is the strain on the matrix, and ε_f is the strain experienced by the fiber. With that said, it can also be said that the total force on the system is the summation of the force on the matrix and the force on the fiber. This is depicted in Figure 2.3. The equation for the total force acting on the composite is

$$F_c = F_m + F_f, \qquad (2.2)$$

where F_m is the force acting on the matrix and F_f is the force acting on the fiber. The total force on the system is directly related to the dimensions of the components by the equation for stress,

$$F = \sigma \cdot A, \qquad (2.3)$$

where σ is the stress and A is the cross-sectional area. Figure 2.3 shows the manner in which the force is exerted on the composite material.

Now that an expression for force has been established, it can be related to strain through an expression known as Hooke's Law [11]. The law links stress and strain by a proportional value known as Young's modulus or the modulus of elasticity

$$E = \frac{\sigma}{\varepsilon}. \qquad (2.4)$$

This equation can be rewritten in terms of force and area

$$E = \frac{F/A}{\varepsilon}, \qquad (2.5)$$

and the force can then be written as

$$F = E \cdot \varepsilon \cdot A, \qquad (2.6a)$$

and the entire force, F_{total}, acting on the composite can be written as

$$F_c = (E_m \cdot \varepsilon \cdot A_m) + (E_f \cdot \varepsilon \cdot A_f), \qquad (2.6b)$$

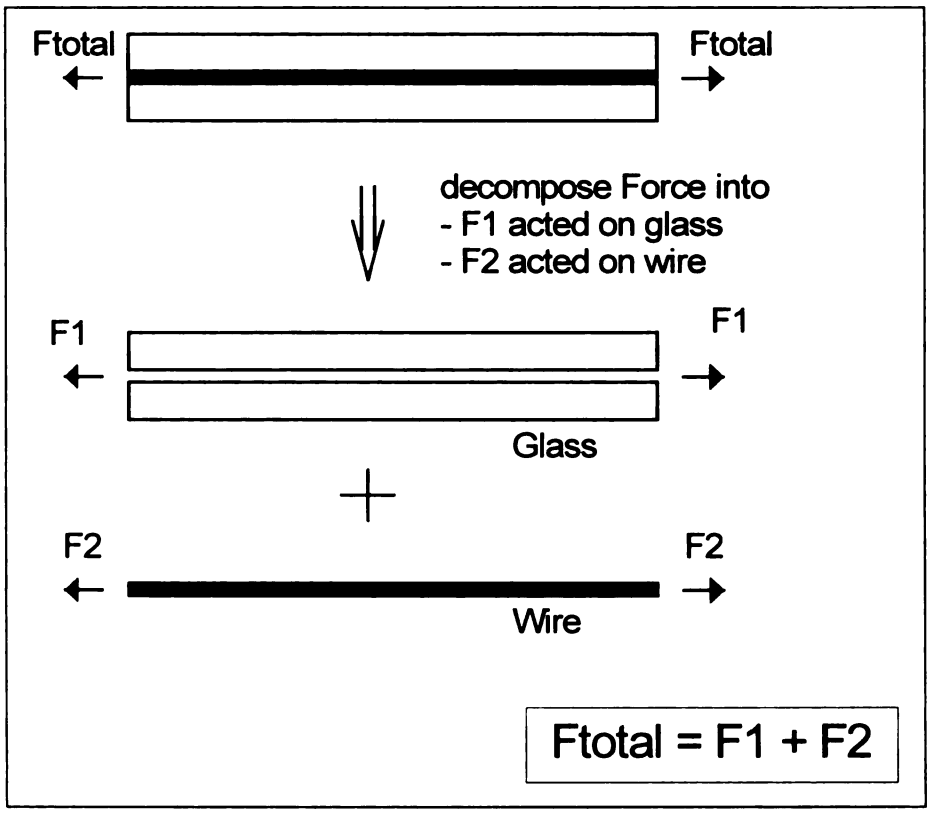

Figure 2.3 Total force acting on composite [10].

Then, substituting Eq. (2.6*b*) into Eq. (2.4), the resulting equation can be reached to determine the elasticity of the composite [12]

$$E_c = \frac{(E_m \cdot A_m + E_f \cdot A_f)\varepsilon / A_c}{\varepsilon}. \qquad (2.7)$$

Because the strain appears on the top and bottom of the equation, it can be cancelled out, which leaves an equation for the elasticity of the composite which is based only on the elasticity of its constituents and their respective dimensions. Thus, if there is a known elasticity that will optimize the probe fabrication process, it can be obtained through the

materials selected and their dimensions. However, this is only a starting point, as it only accounts for behavior at room temperature. The probe fabrication procedure is assisted by a laser, which changes the properties of both the glass matrix and metal reinforcement fiber. It can be used as a reference to what has been accomplished in previous work.

2.1.1 Mechanisms of the Deformation of Fiber-Reinforced Composite in Tension

There are five mechanisms that contribute to deformation in fiber-reinforced composites that are under an axial load. Each stage represents different degrees of stress that the composite is under. The first stage is the elastic deformation stage. Both the fiber and the matrix are bearing the load at this point. Initial crack formation takes place during this stage, but no crack growth [13].

In the second stage of deformation, matrix-fiber debonding begins to occur on a localized level. Also, the matrix begins to experience significant cracking. Matrix-fiber debonding occurs on a wider scale in the third stage, and now the fibers begin to bare the majority of the stress. The entire load is transferred to the fibers in the fourth stage and failure is the fifth stage [13].

The composite featured in this research is a glass matrix and a continuous, single wire, which acts as the reinforcement fiber. This composite goes through each of these stages, however, does so while being struck by a CO_2 laser. The laser is contributing a significant amount of energy to the composite, breaking bonds Si-O bonds of the glass matrix. Eventually, the energy will propagate through the glass matrix and reach the metal wire.

The metal will experience an increase in atomic vibrations when it absorbs the energy of the laser [14]. This affects the plasticity of the metal. As temperature increases, the yield and tensile strengths decrease, and ductility increases (Fig. 3.1). More of this topic is discussed in the next chapter. Thus, the plasticity is improved for both the glass matrix and the metallic reinforcement fiber, a necessary facet considering the extensive amount of plastic deformation that must take place. A way to understand how much the plasticity is affected is to investigate the viscosity of the composite.

2.2 Viscosity of Glass-Metal Composites

Because the matrix of the composite material used is glass, viscosity is a property that must be given consideration. Viscosity, η, is the property that determines fluid flow [13]. More precisely, it can be thought of as the resistance of a substance to flow in a fluid-like behavior. It represents the amount of internal friction present within the fluid when velocity gradients are present. If a fluid is viscous, then it has a higher degree of internal friction and will have a higher resistance to flow. A less viscous fluid will flow easier.

When a micropipette puller draws a glass tube down, it heats the glass and then applies force in tension to pull the glass into two separate pipettes. The heat decreases the viscosity of the glass, so that it will deform in a desired manner. If the viscosity of the glass is not decreased, and tensile force is applied to the glass tube, a brittle fracture will result (Figure 2.4) with practically no strain observed before failure. A large strain before failure is necessary to make a micropipette (Figure 2.5), and this is where the viscous properties of heated glass are of importance.

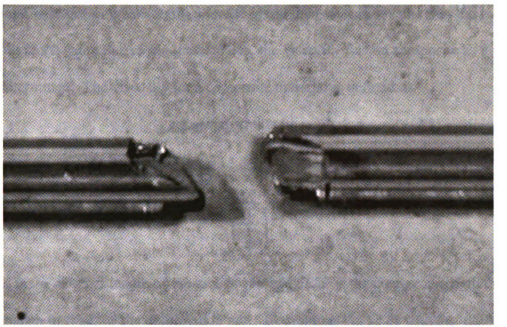

Figure 2.4 Brittle fracture of a borosilicate glass capillary tube that was not heated during deformation. The force was applied axially in tension.

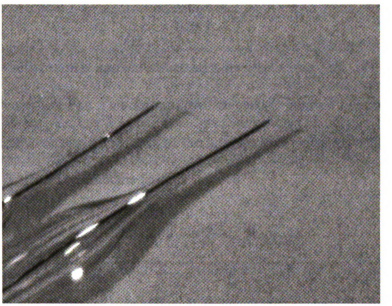

Figure 2.5 Image of glass tube pulled down into a micropipette with a platinum wire inside.

If the metal wire deforms uniformly with the glass, then we can assume that the metal is deforming at the same rate as the glass. Thus, the viscosity for the composite as a whole can be determined. The viscosity for a composite material is defined as

$$\eta = \sigma/\text{strain rate}, \qquad (2.8)$$

and the expression for strain rate is

$$\frac{L_0}{\left(\frac{dL}{dt}\right)}, \qquad (2.9)$$

where L_0 is the original length of the tube or rod and dL/dt is the change in length divided by the change in time, or the deformation rate. Combining Eq. (2.8) with Eq. (2.9) gives a formula for the viscosity of a composite

$$\eta = \frac{\sigma L_0}{\left(\frac{dL}{dt}\right)}, \qquad (2.10)$$

which is a ratio between the applied stress and the strain rate [16, 17]. The units of viscosity are N-sec/m^2, or Pas. This formula will be used to analyze the probe fabrication technique to test how certain parameters of the micropipette puller affect the viscosity of the composite and affect the outcome pull.

3. MATERIAL SELECTION AND EXPERIMENTAL METHOD

3.1 Material Selection

The microprobes (microelectrodes) that were created as a part of this research were fabricated from a glass capillary tube and a thin metal wire. The central difficulty of the microprobe fabrication was inventing a method where, upon application, a glass capillary tube and a thin metal wire inside could be drawn down together simultaneously to form a tapered micropipette that had a conducting metallic channel running to the very tip. This method calls for the uniform deformation of two mechanically different materials, and the microscopic dimensions involved only amplify the level of precision necessary for the success of this method.

The selection of the materials to be used is of utmost importance to the fabrication procedure. Based on research already done in this area, the metal selected should be soft, annealed wire. Therefore we look to the precious metals, known for not only their ductility, but also for their corrosion resistance and excellent electrical conductivity. These properties make metals such as gold and platinum ideal candidates. Metals such as copper and nickel were investigated as well. Table 3.1 lists various materials involved in this research and some relevant physical properties.

The types of glass selected for this research were borosilicate and silica. These are glasses that the micropipette puller used to fabricate the probes was designed for. The ease of fabrication of borosilicate glass makes it preferable to use over silica, however, some of the applications in mind for the probes requires the high melting point and strength of SiO_2. Therefore, both types of glass capillary tubes were experimented with

in conjunction with several different varieties of metal wire. The list of Table 3.1 is the catalog of materials considered for this project, with particular focus on gold, platinum, silica glass, and borosilicate glass.

This section will explain step-by-step the method employed to create micro probes from glass capillary tubing and metal wire. The instrument used to make the probes will be described in detail, along with the integration of the fabricated probes into a scanning probe measurement system.

Table 3.1 List of materials used in research along with select properties.

Material	Elastic Modulus (GPa) at 25 °C	Melting Temp. (°C)	Electrical Resistivity (Ω-cm)
Gold[18]	77.2	1064	2.2×10^{-6}
Nickel[19]	270	1455	6.4×10^{-6}
Copper[18]	110	1083	1.7×10^{-6}
Constantan[18]	162	1300	52.0×10^{-6}
Platinum[18,20]	164.6	1770	10.6×10^{-6}
Platinum/Iridum[18,20]	202.3	1800	25.0×10^{-6}
Platinum/Rhodium[18,20]	212.6	1840	18.8×10^{-6}
Borosilicate[18]	64	800	--
Silica[18,21]	72.9	1410	1×10^{20}

3.1.1 Mechanical Property Considerations

The mechanical properties of the metal wire and glass capillary tube dictated how much force was needed in pulling the pipette into two separate pieces. Through our research, we found that gold and platinum gave the most promising results as the core material for the microprobe. These metals are relatively mechanically soft, with gold at a hardness value of 25 Vickers and platinum at a hardness value of 40 Vickers [18]. These values are obtained with a Vickers Hardness Test that uses a pyramidal shaped indenter, which is made from diamond. Loads of various magnitudes are applied to the surface of the material being tested, and the hardness of the material is based on the diagonal made by the indenter. The Vickers hardness is determined by this equation

$$HV = \frac{1.854F}{D^2}, \qquad (3.1)$$

where F is the applied load and D is the diagonal of the impression made by the indenter (mm) [15].

Intuitively, the softer the material is, the larger D will be, indicating how hard a material is. Generally speaking, the softer a material is, the easier and more uniformly it will deform. In order for a probe tip to be made that has a diameter less than a micron, the wire (initially 50 – 80 μm in diameter) will need to undergo extensive plastic deformation axially. However, the deformation is taking place as a laser is heating the glass and metal. What this requires is that the glass and metal reach a certain viscosity together, so they will draw as a cohesive unit. If the glass and metal are not deforming together simultaneously, a uniform taper will not result.

3.1.2 Temperature Effects on the Mechanical Properties of Metals and Glass

The inherent softness of these precious metals allows for more uniform plastic deformation. Of course, the pulling procedure takes place at elevated temperatures (metals start to lose their mechanical properties at approximately three-quarters of their solidus temperature), softening whatever metal lies inside of the glass, along with the glass itself. Still, it was found that the best probes (finest taper) were of gold and platinum. Figure 3.1 shows the general relationship between mechanical behavior of materials and increasing temperature.

The effect of temperature on metals is complex because not only is there a purely physical effect (the thermal plasticity is related to the amplitude of thermal atomic vibrations which increase when the metal is heated), there are physiochemical process

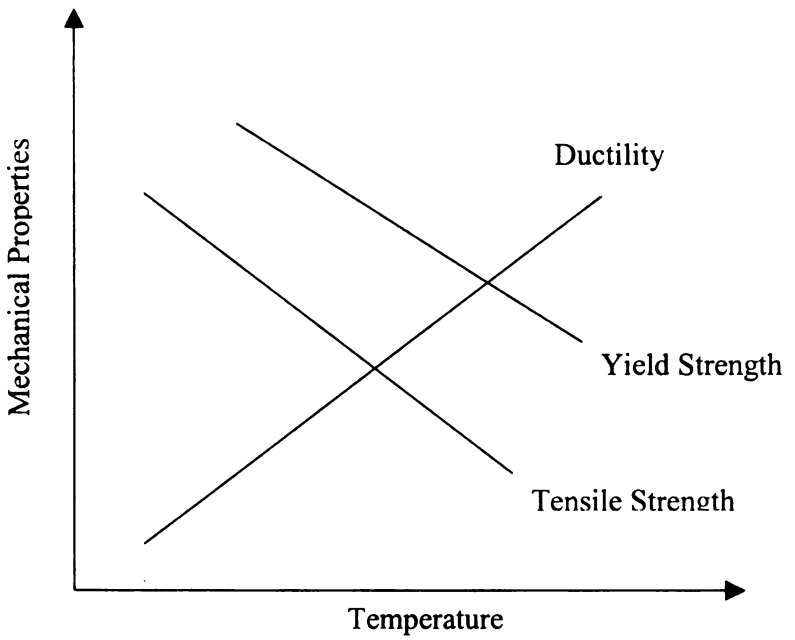

Figure 3.1 Effect of rising temperature vs. mechanical properties of metal [15].

that occur as well . An expression was developed for predicting the effect of temperature on the mechanical properties of metals which is

$$M_2 = M_1 \exp[-\alpha(t_2 - t_1)], \qquad (4.2)$$

where M_1 is a given mechanical property at t_1, M_2 is the resulting mechanical property at t_2, and α is a temperature coefficient of the property [14]. The temperature coefficient takes into account the manner in which the stress is applied, the extent of plastic deformation, the strain rate, etc.

Table 3.2 shows the effect of increasing temperature on some of the mechanical properties of nickel. This table illustrates the effect that temperature has on the properties of metals. Of significance are the tensile strength and the percent elongation. These are important to this type of probe fabrication in that the metal is undergoing extreme plastic

Table 3.2 Temperature dependant mechanical properties of nickel [19].

Temperature (K)	Yield Strength (MPa)	Poisson's Ratio	Tensile Strength (MPa)	Elongation (%)
293	148	0.31	462	47
400	153	0.31	459	46
500	140	0.31	459	44
600	138	0.31	462	46
700	115	0.31	328	64
800	100	0.31	245	68
900	69	0.31	176	72
1000	59	0.31	121	82
1100	45	0.31	83	95

deformation in tension. Figure 3.2 illustrates an example of the decreasing trend in yield and tensile strength and the increasing trend in strain to failure versus increasing

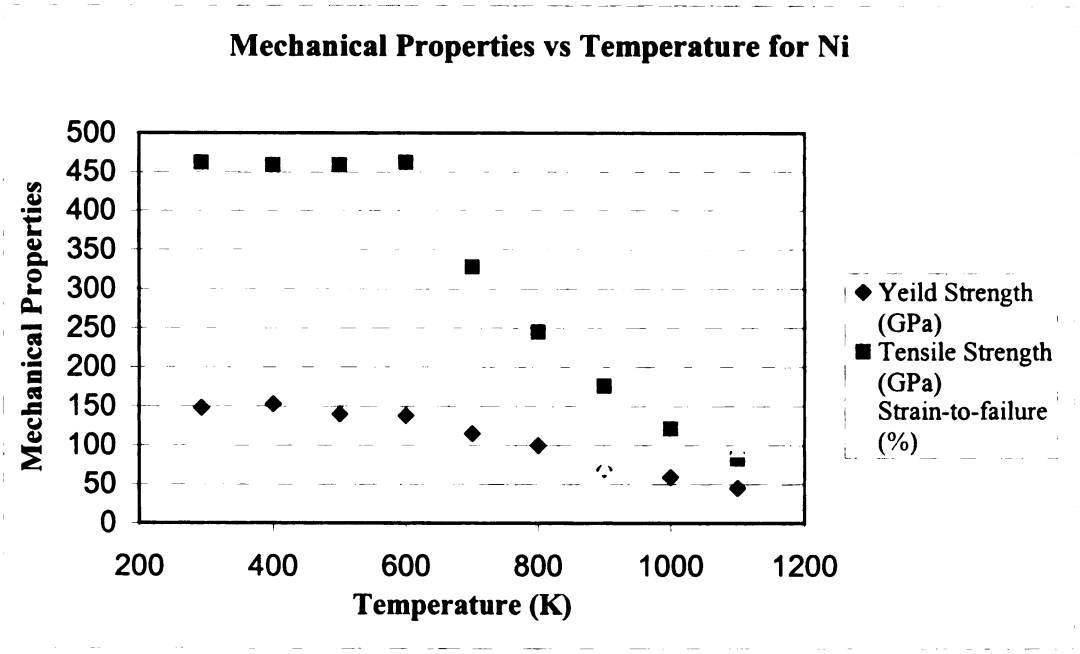

Figure 3.2 Effect of temperature on mechanical properties of nickel [19].

temperature. However, in the actual pulling process the temperature is not known exactly due to the fact that the metal wire is surrounded by glass, so the thermal energy that the metal sees must be estimated.

The mechanical properties of the glass also come into affect, as the glass is the component that dictates the shape of the probe tip. Table 3.3 lists the relationship between mechanical properties and increasing temperature for silica glass. This data shows that the mechanical properties of quartz behave differently from metal under the influence of elevated temperature. The modulus of elasticity, E, increases as temperature increases for silica.

Table 3.3 Temperature dependent mechanical properties of silica glass [22].

Temperature (°C)	Young's Modulus (GPa)	Shear Modulus (GPa)	Poisson's Ratio
25	72.9	31.3	0.165
100	74	31.6	0.171
200	75.1	32	0.173
400	77.2	32.8	0.177
600	78.7	33.3	0.182
800	80	33.7	0.187
1000	81.1	34	0.193
1100	81.4	34.1	0.194
1200	81.5	34.1	0.195
1250	81.4	34	0.197

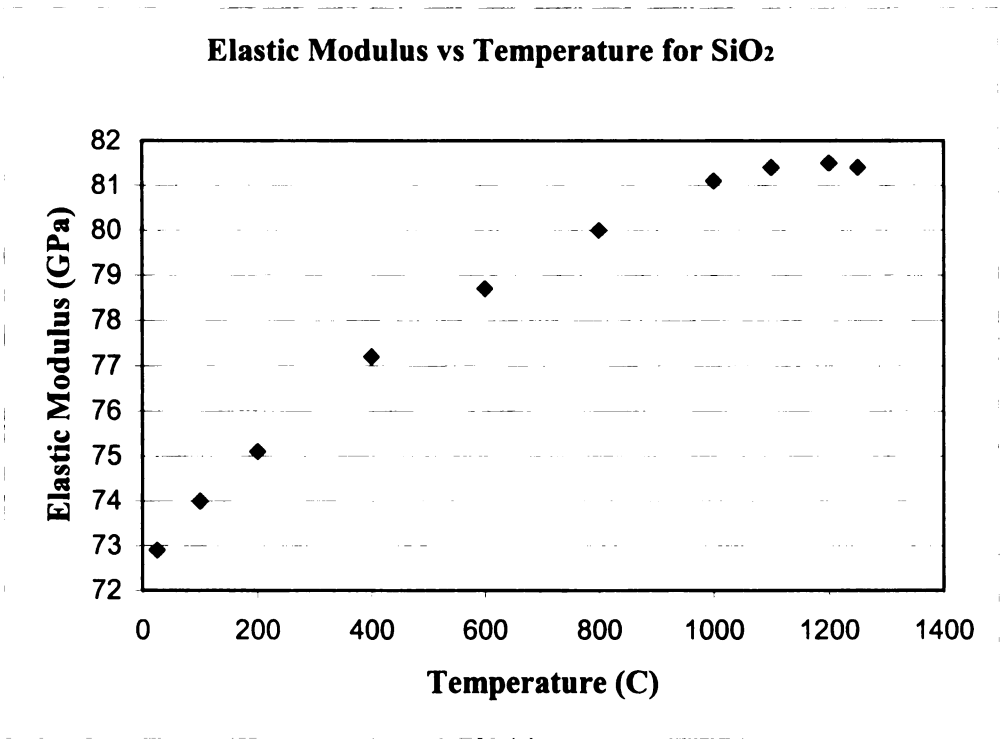

Figure 3.3 Plot of elastic modulus versus increasing temperature for silica glass.

Another property that is affected by temperature is viscosity. The values for viscosity of silica and borosilicate glass are listed in Table 3.4. The values are also listed for increasing temperature. Figure 3.3 plots elastic modulus versus increasing temperature for silica glass and figure 3.4 plots increasing temperature versus viscosity for silica and borosilicate.

Table 3.4 Viscosity versus temperature for silica and borosilicate [22].

	Silica	Borosilicate
Temperature (°C)	Log viscosity (P)	Log viscosity (P)
500	-	15
600	-	12.15
700	-	9.72
800	-	7.88
900	-	6.97
1000	16.8	5.48
1100	14.67	4.74
1200	12.82	4.17
1300	11.21	3.7
1400	9.8	3.4
1600	8.12	-
1800	6.74	-
2000	5.6	-
2200	4.64	-
2400	3.82	-

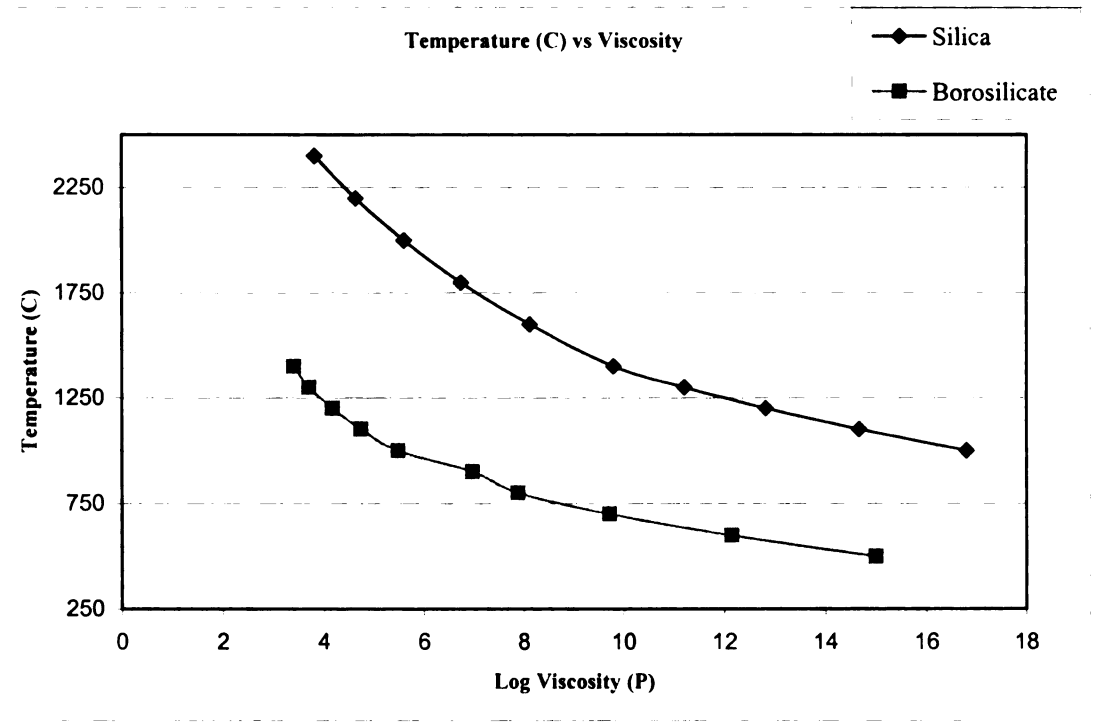

Figure 3.4 Plot of log viscosity versus temperature [22].

From composite material mechanics, it is known that there is a critical volume fraction, V_{cr}, where the plasticity of the composite material becomes equal to the plasticity of the matrix [9]. This helps in selecting the dimensions of the metal wire and the dimensions of the glass capillary tube. The ratio A = D_w/D_{gl} defines the volume fraction V of the reinforcement fiber, where D_w is the diameter of the metal wire and D_{gl} is the outside diameter of the glass tube [9]. Therefore, by holding the diameter of the wire constant, the outer diameter of the glass can be varied to reach a point where $V \approx V_{cr}$ [9]. *Nanonics* [2, 9] reported the best results for volume fractions between 0.2 and 0.4 for platinum wire and borosilicate glass. An analysis of the mechanics of the platinum and borosilicate pulling procedure can be seen in Chapter 2.

Another factor to consider is how the metal and glass properties compare to one another. Referring back to Table 3.1, gold and borosilicate glass share similar properties mechanically and thermally. Of course, the plasticity of gold and borosilicate differ greatly, borosilicate glass being very brittle and gold being ductile. However, the melting points of the two are quite similar and actually were very useful to us for this study.

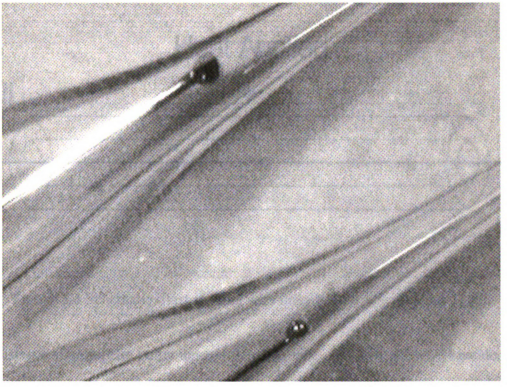

Figure 3.5 Wire melted inside pulled micropipette.

An example of a poor match of glass and metal can be seen in figure 3.5. Using gold with silica does not work well because the melting point of gold is far less than even the softening point of silica. Therefore, the gold will melt inside the tube before the silica begins to pull, which does not give gold the chance to pull simultaneously with the silica.

3.2 Probe Fabrication

The probe fabrication technique developed for this research was based on previous works mentioned in the introduction [1,2,3]. They devised a method in which a metal wire (gold, platinum, silver, etc.) was inserted into a capillary tube of borosilicate glass. This step is depicted in Figure 3.6.

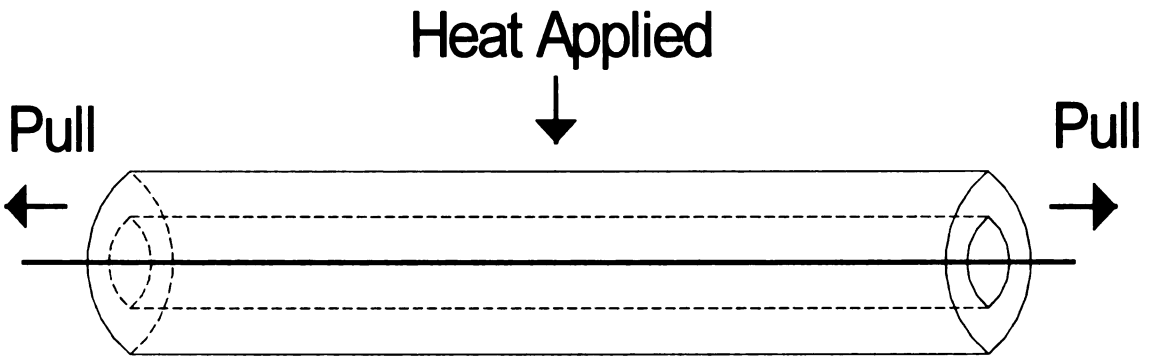

Figure 3.6 Schematic illustration of wire threaded through glass tube [10].

Then using a micropipette puller tapered the glass tube, along with the wire inside, down into two separate pieces. Figure 3.7 depicts the probes created by the micropipette puller, noting the great deal of tapering near the tips.

The puller works by heating the center of the tube and pulling on each end of the tube to taper the glass. One could pull hundreds of tubes down into micropipettes a day, it is a very simple task given a capable puller. However, these pullers are not designed to create micropipettes from the glass tube including the wire, which is why a very specific technique must be developed through experimental methods.

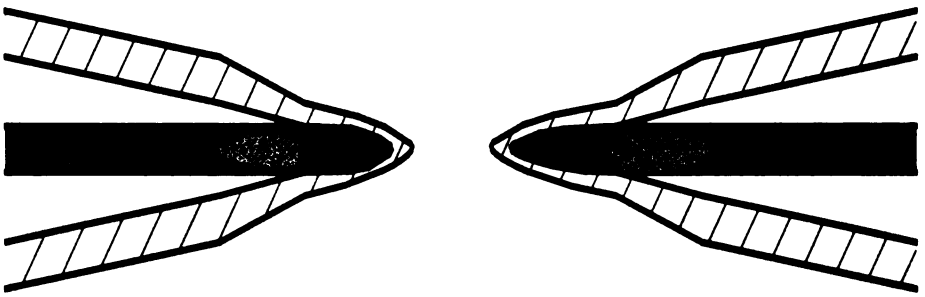

Figure 3.7 Resulting probe tip shape from the fabrication procedure [10].

The micropipette is a useful instrument and, as mentioned in previous sections, finds many applications in biological research and now more commonly in other branches of scientific research. The unique properties of glass allow for such a simple process to produce a powerful instrument. The glass, in the case of a micropipette probe acts as the matrix for the metal wire if the combination is thought of as a composite material.

A metal wire could not be fashioned this sharp and precise by any other physical material reduction method while at the same time creating an insulated covering for the metallic core. The glass forms as it would and induces the metal wire to form along with it. This requires the glass and the metal to have a certain degree of viscosity. The wire is undergoing extensive plastic deformation, as there have been metal tips reported with diameters less than 50 nm from a wire that was originally 50 μm, a 1000% reduction in diameter [9]. This is no trivial matter, as a 50 μm wire is very sensitive to breaking and melting. A small tear or separation of the wire near the tip can significantly affect the

ability of the probe to conduct electricity. Measures can be taken, however, to aid the deformation procedure.

3.2.1 Sutter P-2000 Micropipette Puller

The Sutter P-2000 (Figure 3.8) uses several parameters to deliver the proper amount of heat, force, and timing to fashion a micropipette, or in this case, a probe with a micron

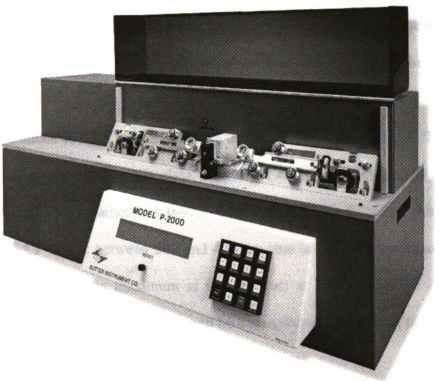

Figure 3.8 Sutter P-2000 micropipette puller [23].

scale tip diameter. A CO_2 laser supplies the heat and was selected for this micropipette puller for several reasons. The wavelength of this type of laser matches the resonant frequency of the silica lattice, allowing the fabrication of pipettes out of silica. There is

no metal residue on the pipette because of clean heat delivered by the laser. Finally, laser heat can be turned off instantly, leaving no residual filament heat.

This is advantageous in that many pipettes can be fabricated in a relatively short amount of time with little or no waste produced. Once a program to create the micro probes is established, a large quantity of them can be made shortly. However, the reproducibility of each pull is an issue. A pulling program may work well one time, then fail to reproduce those results for several attempts. There are many factors that affect the reproducibility of each pull, for example, the way in which the wire is placed in the glass tube, whether or not the mirror is clean, whether or not the glass tube is of correct dimension, etc.

The first parameter is HEAT, which dictates the output power of the laser. The energy of the laser will be absorbed by the glass, which will soften once adequately heated. The range of the HEAT parameter is 0-999, with 500-600 able to soften thin wall silica tubing. HEAT values between 300 and 400 are able to soften borosilicate glass [24]. Laser power is 10 Watts maximum at 999, 0 Watt at 100 and can be calculated as Watts=(HEAT-100)/ 90. Temperature will be a complicated function of the HEAT value, time, the glass size and other factors.

The next parameter is the FILAMENT. The FILAMENT selects the scanning pattern of the laser beam. The range of this parameter is 0-15, which defines the length of the scanning pattern in millimeters; a value of 1 would produce a 1 mm scanning length, a value of 2 would give a 2 mm scanning length, etc. Figure 3.9 shows an example of the display where the parameters are entered [24].

HEAT	FILAMENT	VELOCITY	DELAY	PULL
600	4	55	128	70

Figure 3.9 Sample of the display where the program is entered into the P-2000.

The VELOCITY specifies a certain glass temperature to trigger the hard pull. The rate at which the clamps move apart is measured as the glass softens and begins to stretch. This increasing velocity is related to the viscosity of the glass, which is a function of the glass temperature. The range of this parameter is 0-255 with useful values falling between 10 and 100, with units of millivolts of transducer output. If the VELOCITY value is too high, the glass will separate before the pull [24].

The PULL is the parameter that controls the force of the hard pull on the glass. The total pull force acting on the glass comes from a slight gravity pull and the force programmed into the micropipette puller. Thus, the total pull force is made up of these two parts.

The glass carrier bars (Figure 3.10) are attached to cables that are brought by pulleys to a common point of attachment on the plunger of a solenoid, which is the source of the weak gravitational force mentioned above. When the glass tube is loaded into the carrier bars, the bars are brought close together, lifting the plunger. The weight of this plunger along with all of the components is approximately 0.171 kg [24].

The programmable force is produced by passing current through the coil of the solenoid. The current is turned on at after the velocity value has been reached. The current that is supplied to the solenoid is based on the PULL value; a value of 255 sends 2.5 amps. For a pull value of 221, the load applied is 53 lb.

The DELAY parameter dictates the amount of time between the shutting off of the heat (the CO_2 laser), and the initiation of the hard pull. This allows for time to allow the glass to cool a bit. Using a high delay value will generally result in a shorter taper length and a larger tip diameter. The range for this parameter is 0-255 and the units are milliseconds. The default setting for this parameter is set at 128. At this value, the hard pull will activate at the same time as the deactivation of the laser beam. If a value greater

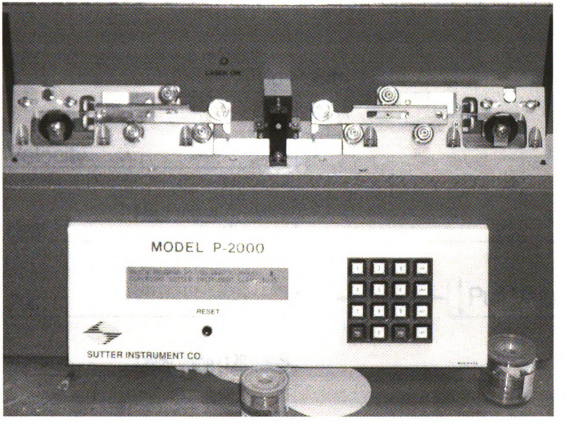

Figure 3.10 Image of the carriage system of the P-2000.

than 128 is used, the hard pull will be initiated after the laser turns off. Similarly, if a value less than 128 is chosen, the hard pull will begin before the deactivation of the laser [24].

Much of the early experimentation with the P-2000 involved testing how each parameter affected the size and shape of the tip. This testing began on pipettes without a metal wire inside. Four of the parameters would be held constant while the fifth was varied throughout its range of values. After obtaining a rough feel for each parameter, several different metals were selected to use as the electrical conducting core for the probe. The metals were chosen based on their physical properties and what had been experimented with in previous studies.

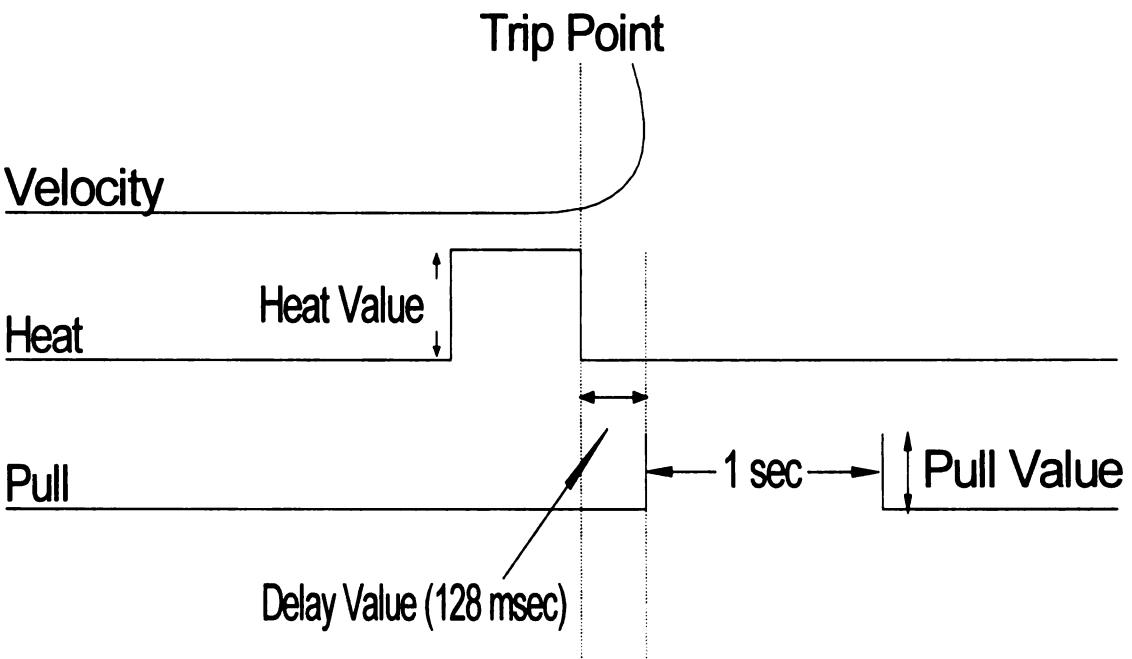

Figure 3.11 Pull cycle when a DELAY greater than 128 is selected [24].

The VELOCITY and DELAY parameters dictate the timing of the pull as illustrated in Figures 3.11 and 3.12. The VELOCITY determines the point at which the laser turns off. The DELAY is the time between the laser deactivation and the PULL activation. Therefore, if no DELAY is used in a given program, the pull will initiate as

soon as a certain viscosity is reached. Likewise, if a DELAY of less than 128 is used, the pull will begin before the laser is deactivated.

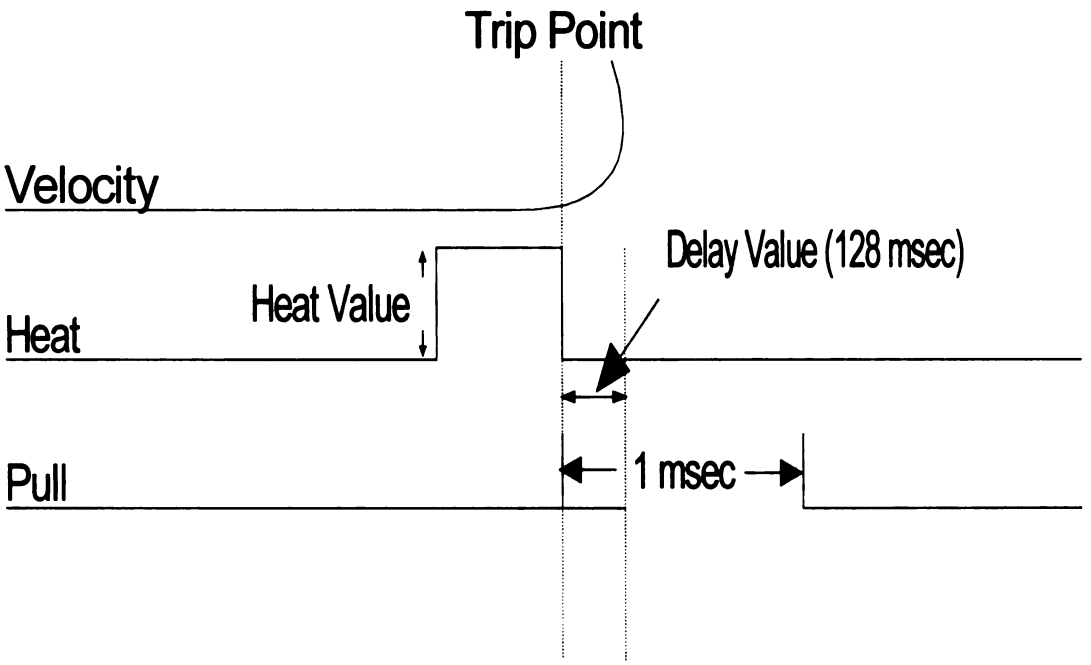

Figure 3.12 Pull cycle when a DELAY less than 128 is selected [24].

3.3 Micro Probe Fabrication Method

Before extensive testing with the metal wire began however, a manipulation of the glass tube was needed. As seen in the sketch, figure 3.13, a large dimensional gap exists between the inner wall of the glass tube and the metal wire. The micropipette puller is optimized for pulling glass tubing that has an outer diameter of 1.0 mm. Through the preliminary experimentation, capillary tubing with 1.0 mm outer diameter and 0.5 mm inside diameter was settled on, although silica tubes with 1.0 mm outer diameter and 0.3 mm inner diameter were tested as well, with varying degrees of success. Inserting a 50 μm wire inside of a tube with 0.5 mm inner diameter leaves a significant

gap between the wire and glass.

A problem arises for several reasons because of this dimensional mismatch. First, air is an excellent insulator of thermal energy. If the air is absorbing most of the energy from the laser, the wire will not receive enough energy necessary to soften and alter its

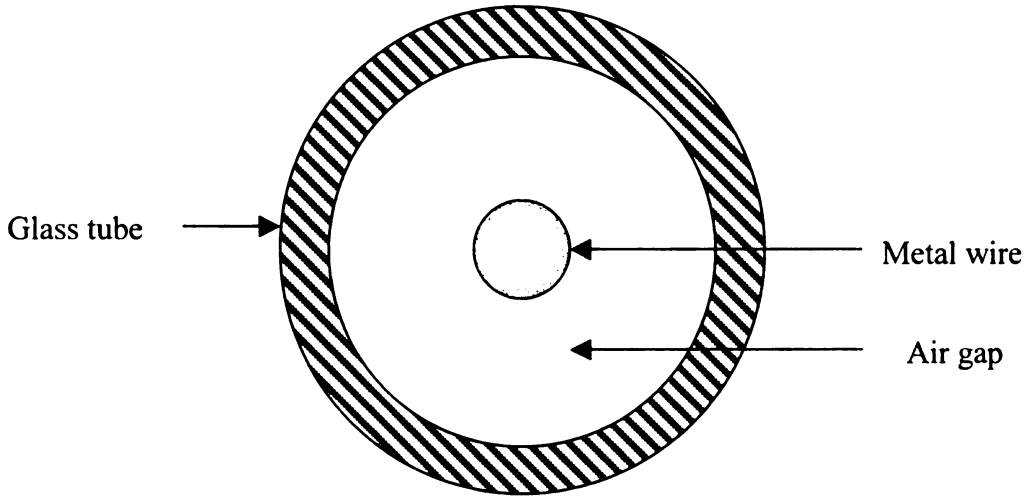

Figure 3.13 Sketch of cross-sectional view of the dimensional mismatch between the inner wall of glass capillary tube and the metal wire.

mechanical properties. When the force of the pull is exerted on the wire without sufficient heating, the wire will snap and result in two flat ends rather than a gradual taper to a fine point. The first step would be to reduce the dimensional mismatch between the inner wall of the glass tube and the metal wire. Figure 3.14 shows one of the several results that can occur from bypassing the first step.

In the article by Fish, et al. [9], they recommend breaking the pulling procedure down into two or three steps. The first step is to pull the glass down far enough that the

inner diameter of the tube is the same as the diameter of the wire (Figure 3.15). A specific program was designed to perform this task.

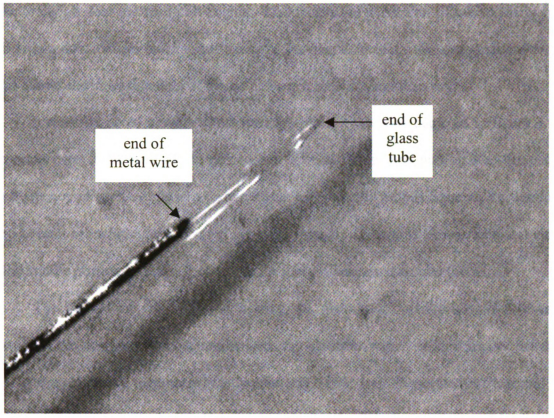

Figure 3.14 Example of microprobe that was pulled with the wire breaking prematurely. As seen, the tapered glass extends far beyond the point where the wire ended.

One program, designed for 1.0 mm outside diameter, 0.5 inside diameter borosilicate glass and 0.05 mm gold wire, called for

- Heat – 400
- Filament – 4
- Velocity – 50
- Delay – 200
- Pull – 20

This program was designed for 1.0 mm outside diameter, 0.5 mm inside diameter borosilicate glass and 0.05 mm gold wire. The DELAY value of 200 gives the glass 72 msec to cool before the hard pull begins. This means the glass won't flow so easily and will regain some of its mechanical strength, leaving it in tact. Also, a smaller PULL force allows the inner diameter of the tube to reach the wire and then stop.

It must be noted however, that instances such as the one depicted in figure 3.14 can occur even if the first step is carried out. Executing the first pulling step decreases the frequency of such events to a certain extent and the only probes deemed "successful" were a result of including the first pulling step. Figure 3.16 depicts a cross sectional view of the middle portion of figure 3.15 where the glass is collapsed around the wire.

The second step is simply a heating the glass/metal combination for several seconds to provide better connection between the glass and metal. It is important that the glass and metal move together when they deform. That way, the amount of tapering of the metal wire is maximized. However, through significant experimentation, it was concluded that this step is not always necessary.

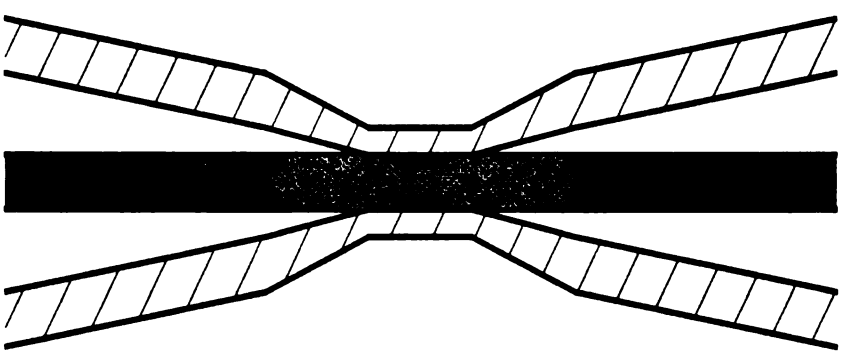

Figure 3.15 Glass tube collapsed around the metal wire as the first pulling step in the probe fabrication procedure [10].

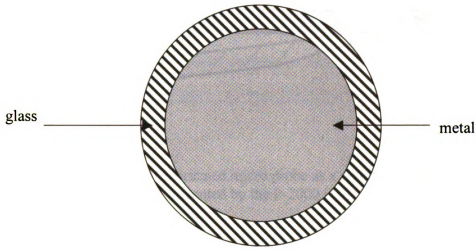

Figure 3.16 Cross-sectional view of middle portion of Figure 3.15. The glass is pulled down so that the air gap that existed between the glass and the metal is either minimal or eliminated completely.

The third step in the procedure is the final pulling step, which is the most difficult to program. The desired result will look similar to the sketch of Figure 3.17. After the final step, if the pull appeared successful (the metal wire was continuous to the very end of the tip), the very tip of the glass was etched with hydrofluoric acid (HF).

The preliminary observation of the probe was done under an optical microscope, making it extremely difficult to see the tip of the probe, even more difficult to determine if there was a thin coating of glass covering the metallic tip. Even the thinnest coating of glass could render the probe useless, particularly if the use of the probe requires that it conduct electricity. Therefore, the tips of the pipette were given an HF bath to remove any glass that may have covered the metal.

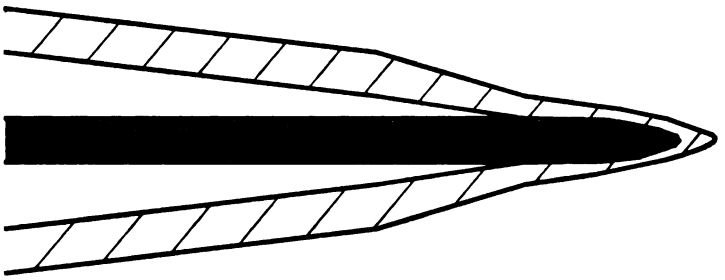

Figure 3.17 Illustration of fabricated micro probe as a result of the pulling procedure executed by the P-2000 [10].

The HF bath consisted of one part 50% HF and six parts H_2O. This gave a solution with a glass-etching rate of approximately 120 nm/min. A bath of about two minutes was adequate for most of the pulled probes, yet sometimes the probes were exposed to the HF for longer periods of time to ensure an appropriate amount of etching would occur. Only the tip was dipped into the HF bath.

Unfortunately, there was no direct way to observe if all of the glass had been removed from the tip of the probe. The only way to determine this was by viewing the sample in a scanning electron microscope (SEM). If there was no charging at the tip, it was assumed that the glass had been removed.

3.4 Probe Measurement Technique

Once fabricated, the probes were viewed under a SEM to determine if indeed the metal wire was continuous to the very tip of the pipette and all of the glass had been removed

during the HF etching procedure. If so, the probe was integrated into a four-point probe arrangement.

In a traditional four-point probe set-up, there are two leads for current and two electrodes for voltage drop measurement. This is demonstrated in Fig 3.18. In this configuration, the probes that measure the voltage drop are held at a constant spacing, *l*, from each other. This spacing allows for the calculation of electrical conductivity in the sample from the expression

$$\sigma = \frac{Il}{VA}, \qquad (3.2)$$

where, σ is the electrical conductivity, I is the amount of current passed through the sample, V is the voltage, and A is the cross-sectional area of the sample.

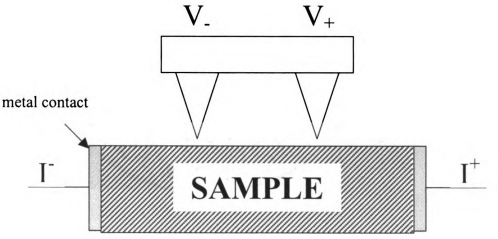

Figure 3.18 Schematic of traditional four-point probe arrangement.

What we altered as part of our project was moving V. to the electrode that I. is using. Then, we mounted V_+ (our fabricated microelectrode) onto a *xyz* translational stage so that it is free to scan the entire surface of the sample. The current leads were

connected to the sample through metal contacts on the sample. These contacts were put on the sample through sputter coating, metal evaporation, or electrochemical deposition. This creates a contact resistance at these points. Because our probe is free to translate, the contact potential at the metal contact can be measured, and then added to the measured voltage drop. This is advantageous over the traditional four-point probe because of this ability to measure the contact resistance.

Figure 3.19 shows a schematic of the scanning one-probe setup. The current leads are connected to a Keithley 2400 source meter, which was set to deliver 10 mA across the sample. The voltage probes were run to the Keithley 2182 nanovoltmeter to record the voltage drop across the sample [10].

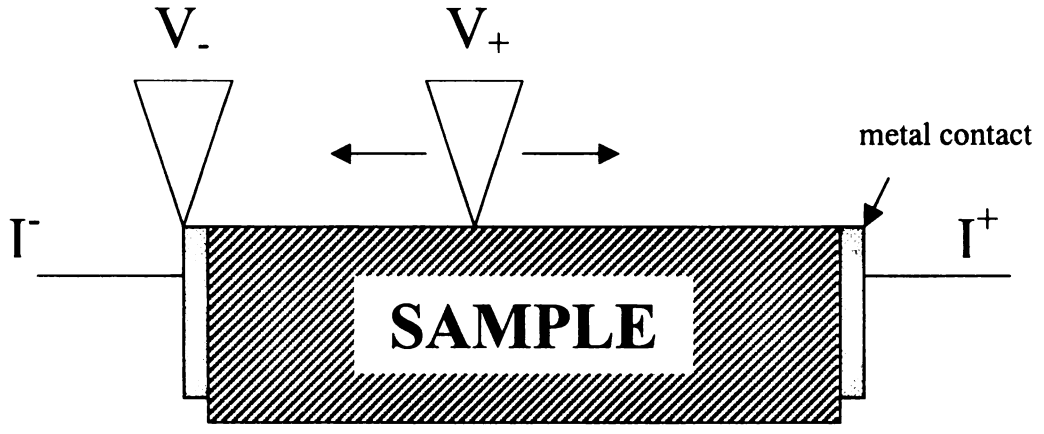

Figure 3.19 Illustration of one-point scanning probe setup. The micro probe is mounted on a *xyz* transnational stage and acts as the positive voltage probe. This probe is free to scan over the entire surface of the sample.

The basic methodology of the experiment using this arrangement is to first measure the resistance one end of the sample where the contact has been deposited. Then, the scanning probe is moved toward the opposite end of the sample and the voltage

drop changes in accordance with the increased probe spacing between V_- and V_+. This procedure will be discussed further in the Results portion of the write up.

4. RESULTS

4.1 Probe Fabrication

Microprobes were fabricated from glass capillary tubes and metal wires. The goal of the fabrication process was to create a probe that had as small of a tip as possible. Desirable results of the tip diameter were on the order of 1 μm and below. Also, it was imperative that the wire be continuous to the very end of the tip, for purposes of conducting electricity. The results for the fabrication of micro probes from gold and platinum showed promise. Some of the other metals, however, proved more difficult to create the probe tips that were of the desired tip diameter.

The design of the pulling procedures will be presented in this chapter, along with results of the probe fabrication and the conductivity measurements done with platinum microelectrodes. The probes were integrated into a variation of the four-point probe configuration, where the micro probe acted as a scanning electrode. Conductivity measurements were conducted across the surface of the sample to test the effectiveness of the fabricated micro probes as electrodes.

Images of the probes will be presented along with the pulling procedure for each. Each pulling procedure consists of three steps and produces two micro probes. The first step, after the wire is inserted into the glass tube, is to collapse the glass down around the wire (Figure 3.15). The second step is a heating only step, to ensure a good mechanical bond between the glass and metal. The third step is the final step, where the heat and pull are such that the glass and metal are pulled apart (Fig. 3.7).

4.1.1 Critical Volume Fraction

Will the glass matrix and metal wire behave and deform together as a composite material? These are two materials that have distinctly different mechanical behavior, yet in the proper volume fractions, the desired mechanical behavior for the composite is possible. There is a critical volume, V_{cr}, where the plasticity of the composite material becomes equal to the plasticity of the matrix [9]. The volume fraction, A, of the wire can be defined as

$$A = \frac{d_f}{d_m}, \qquad (4.1)$$

where d_f is the diameter of the wire and d_m is the outer diameter of the glass tube.

It is actually the thickness of the glass tube that is of significance. The article from The Hebrew University of Jerusalem [9] describes a particular glass-metal combination they used to make microprobes. Using 0.08 mm platinum wire, annealed, and 1.2 mm outer diameter, 0.3 mm inner diameter, they executed the step to collapse the glass tube around the metal wire. Therefore, the inner diameter of the glass becomes 0.08 mm and the outer diameter of the tube becomes 0.32 mm, as can be seen in Fig. 2.2.

For this particular glass-metal combination, the authors reported pulling tips as small as 50 nm in diameter. They state that this is possible for tube and wire and glass dimensions where $0.2 < A < 0.4$. For the dimensions mentioned above, $A = 0.25$. Of course, there is a specific pulling program that must be designed for this glass tube and metal wire composite. This same critical volume value would not necessarily work the

same if the glass used was silica rather than borosilicate, or if the metal was not platinum, but silver instead.

This critical volume fraction ratio simply gives a starting point, helping to determine the dimensions of the glass and metal that can work well together in the fabrication procedure. At the critical volume fraction of the fiber, as stated above, the plasticity of the matrix represents the plasticity of the entire composite [9].

4.1.2 Fabrication of Microprobes from a Borosilicate Glass Tube and Pt Wire

This combination of glass and metal had a very large mismatch in physical properties. The melting point of platinum is above 1400° C whereas the melting point of borosilicate glass is closer to 1100° C approximately. This made the first step very simple; the borosilicate glass was easily pulled down around the platinum wire without the wire weakening at all. In the second step however, because the glass is already weakened, the high heat needed to melt the platinum wire inside was too much for the glass to handle.

Using 1.0 mm outer diameter, 0.5 mm inner diameter along with 0.05 mm platinum wire, the glass was pulled down around the wire. Then several different programs were experimented with, all of them resulting in poor results. Heat values ranging from 600 – 900 and each value of filament was tested. The pull values were left small, as well as the velocity. The delay values were kept high, to hold intact the integrity of the glass as long as possible.

What was found in every case besides those where the heat was set to a very high value (above 800) is that the glass would separate but the wire would not. In the

cases of high heat, the combination of glass and metal would pull, but it would not form a small tapered tip that could be useful as a submicron probe. Instead it would usually form a flat, broad tip.

Further experimentation with this combination could lead to more promising results, as *Nanonics* and the Hebrew University of Jerusalem reported fabricating similar probes with these two specific materials and the Sutter P2000 [9]. However, *Nanonics* used specific dimensions where the volume fraction of the composite was between 0.2 and 0.4. Under these conditions, they pulled probes with tip diameters of 50 nm.

4.1.3 Fabrication of Microprobes from a Silica Tube and Pt Wire

The melting points of platinum and silica are significantly closer than that of platinum and borosilicate. Therefore, this combination was explored a bit more comprehensively than the glass/metal combinations that have been discussed already, even though it seems that the relative dimensions of the matrix and fiber are more important than their respective physical properties. Some of the potential applications for the probes call for service temperatures above the softening point of borosilicate glass. For certain applications, then, silica would be required as the matrix material.

The first trial was carried out with 1.0 mm outer diameter, 0.3 mm inner diameter silica glass and 0.08 mm diameter annealed Pt wire. The $0.2 < A < 0.4$ guideline [ultrafast] was not purposely followed in this case because we were no longer dealing with borosilicate glass. However, for these dimensions, the volume fraction of glass to metal was 0.3, and promising results were obtained.

For this pulling procedure, first the platinum wire was inserted into the quarts tube. Then, the following program was used to pull the tube down around the wire:

- Heat – 720
- Filament – 5
- Velocity – 50
- Delay – 250
- Pull – 145

This program used a high heat value to soften the silica, and a high delay value (122 msec before the pull was initiated) to give the glass a moment to recover and not separate completely, but instead only stretch. A high pull value was required as well to stretch the silica. The result of this step is seen in figure 4.1.

Because of the geometry of the tube and wire, this step only had to be run one time (the tube did not need to be stretched very extensively because the inner diameter of the tube was 300 microns and the diameter of the wire was 80 microns, therefore only about a 200 micron gap had to be closed between the glass and the metal).

This was enough to collapse the glass around the Pt wire and eliminate most of the gap that existed between the inner diameter of the tube and the Pt wire. Then, the program was executed to heat – but not pull – the glass and metal. This step was executed in an attempt to achieve a stronger bond at the interface of the two materials. After this step was completed, the final pulling step was initiated. This step called for the following program:

- Heat – 650
- Filament – 5

- Velocity – 50
- Delay – 100
- Pull – 100

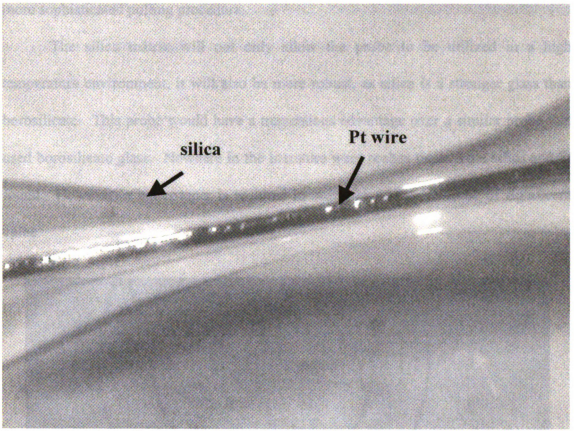

Figure 4.1 First pulling step of 0.3 mm inner diameter silica tube and 0.08 mm Pt wire.

A high heat value was employed for this step to soften the silica and the Pt so they would taper finely during the hard pull. The pull will activate for 28 msec while the laser is still on, then the laser will turn off as the pull continues. Therefore, part of the pull is taking place while the glass and metal are at their hottest points. This should be the best time for the pull to take place because both the glass and the metal should be in their most readily deformable states.

This program yielded the result depicted in Figure 4.2. The diameter of the tip was less than 20 microns, relatively speaking not a desirable outcome. However, the outcome of this pull exhibited a very nice taper, and encouraging sign for developing a more sophisticated pulling procedure.

The silica matrix will not only allow the probe to be utilized in a high temperature environment, it will also be more robust, as silica is a stronger glass than borosilicate. This probe would have a tremendous advantage over a similar probe that used borosilicate glass. Nowhere in the literature were probes made from silica and Pt found. However, a better taper is required in order for this probe to be of significant value.

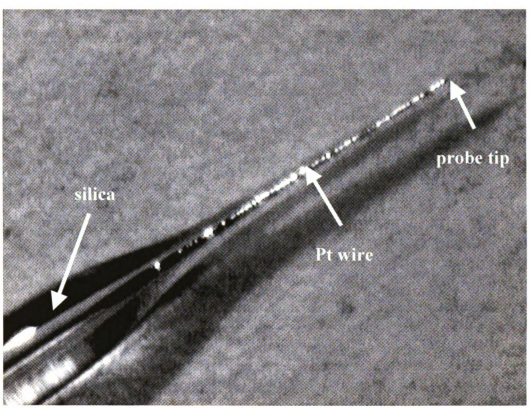

Figure 4.2 Result of pull with 0.3 mm inner diameter silica tube and 0.08 mm diameter Pt wire. The diameter of the tip is approximately 0.02 mm.

Several variations of this program were investigated. Another tip that was produced was fabricated using the same initial step to collapse the glass around the wire. The second step was altered however, using a higher heat, lower filament, same velocity, higher delay, and smaller pulling force. This was done to give the metal wire a slightly longer time to soften so the tip would have a smaller diameter. The program goes as follows:

- Heat – 850
- Filament – 4
- Velocity – 50
- Delay – 135
- Pull – 80

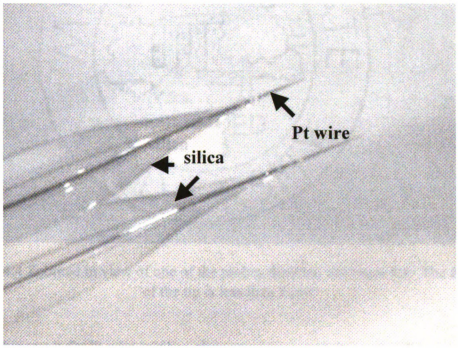

Figure 4.3 Image of probes made of 0.3 mm inner diameter silica glass and 50 μm Pt wire.

This program yielded another good result as can be seen in Figure 4.3. Many programs leading up to this image produced poor results. Each program was tweaked and tuned until a good result was obtained. A good result is one where the taper is fine and the wire is pulled to the very end, as seen in Figure 4.4. A 50 μm Pt wire was used for the probes seen in Figures 4.3 and 4.4 along with 1.0 mm outer diameter, 0.3 mm inner diameter silica tubing. The critical volume fraction then became 0.3.

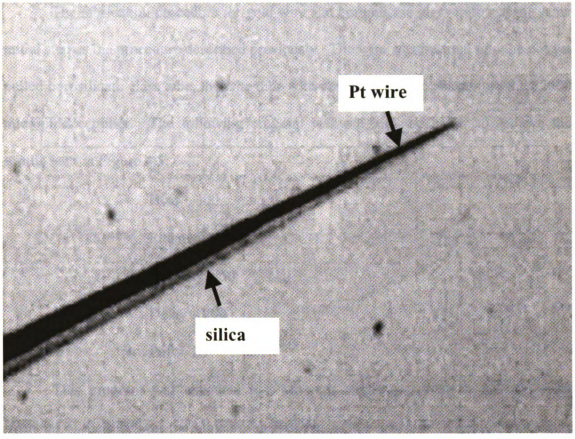

Figure 4.4 Zoomed in view of one of the probes depicted in Figure 4.3. The diameter of the tip is less than 5 μm.

This result for Pt wire in silica glass was very promising and with more variation of the program, a smaller, more finely tapered tip could result. This was an improvement over the result obtained in Figure 4.2

4.1.4 Fabrication of Microprobes from a Borosilicate Glass Tube and Au Wire

This glass and metal combination worked the best for creating micro probes. The dimensions of the materials were 1.0 mm outer diameter, 0.5 mm inner diameter for the borosilicate tube, and 0.05 mm diameter gold wire. The pulling procedure, results of the pulling procedure, and the measurements taken using the probe will be presented in this section. The volume fraction for this glass-metal composite is 0.5.

The fabrication procedure for gold wire and borosilicate glass followed the same initial step as the procedure described previously. The wire was inserted into the not yet pulled borosilicate glass tube, then the tube with wire inside were placed into the P2000 micropipette puller. The following program was put into the puller to achieve the results seen in Figure 4.5:

- Heat – 400
- Filament – 4
- Velocity – 50
- Delay – 200
- Pull – 20

This program was executed two times to stretch the tube so that the inner diameter of the tube was the same as the diameter of the gold wire. Again, a high delay was used to allow for recovery of the softened glass for a brief time period so that only stretching of the tube occurs, and not separation. A small pull value was employed as well so the glass will not pull apart.

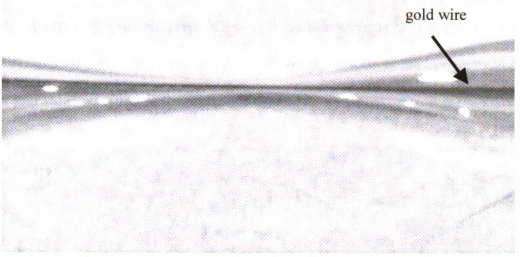

Figure 4.5 Initial pull that shows a borosilicate tube pulled down around a gold wire.

At this point a different step was executed that had not been used in any of the previous pulls. One side of the tube was unclamped and the entire pipette is shifted over a couple of millimeters and then clamped again. Figure 4.6 illustrates where the laser would hit before the pipette was shifted and approximately where the laser beam strikes the pipette after the shift. Figures 4.7a and 4.7b show the difference of the results of the final pull with and without the shift.

The shift was done right before the final pulling step and our best results were obtained when this step in the pulling procedure was employed. The final pull program was:

- Heat – 370
- Filament – 4

- Velocity – 40
- Delay – 0
- Pull – 65

A smaller heat value than what was used in the initial pull was used because the gold wire touched the borosilicate glass, allowing more heat to transfer directly to the wire. A delay value of zero was used so the pull will initiate as soon as the laser activated. A larger pull value was used so the probe tips tapered down extensively. It is not known

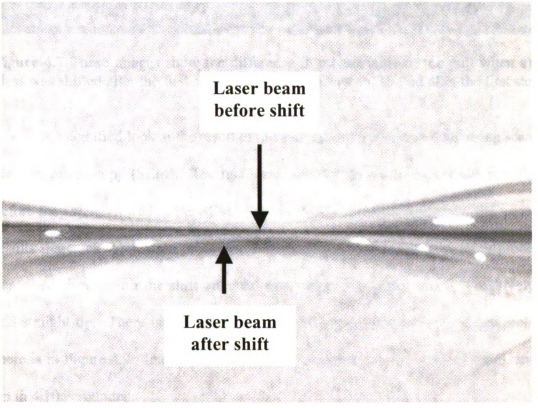

Figure 4.6 This figure illustrates where the laser beam would strike the glass normally and where it strikes the tube after it has been shifted over.

exactly why shifting the glass over a few millimeters makes such a dramatic difference in the outcome of pulling procedure. Most likely, the gold wire is well gripped by the

glass to the right of where the laser beam strikes, and the result is a very finely tapered tip with gold continuous to the very end.

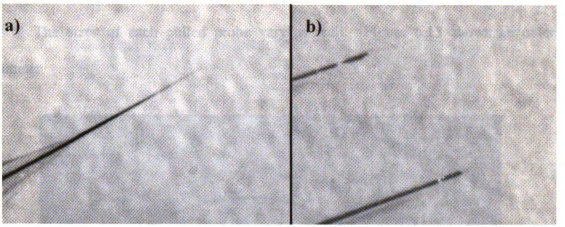

Figure 4.7 These images show the difference in the outcome of the pull when a). the glass was shifted after the first step and b) the glass was not shifted after the first step.

A magnified look at the result of this pulling procedure was done using scanning electron microscopy (SEM). The tips were etched with HF to expose the metallic tip before they were viewed in the SEM. Several different images will show the variety of results that each fabrication procedure can yield (each using the fabrication procedure described above, with the shift after the first step). Figure 4.8 shows a relatively flat and straight tip. There is not, however, extensive tapering at the end of this probe, as there is in Figure 4.9. Interestingly, the tip in 4.8 is flat, the tip in 4.9 is sharp, and the tip in 4.10 is rounded.

Each probe in Figures 4.8, 4.9, and 4.10 was pulled with the same pulling program that included the glass shift. It is clearly seen how each pull varies, especially at the micrometer level. Each tip has a different outer diameter, and shape. There are several possibilities as to why each pulled tip has such variation, including how the glass and metal were mounted in the micropipette puller (wire was kinked inside glass

tube), contaminants on the surface of the glass during the pull, minute differences in the pull force, etc. In an extremely sensitive fabrication process such as this, the smallest variations can lead to dramatic changes in the result.

The sizes of each pulled probe vary as well. Figure 6.13 shows an outer diameter

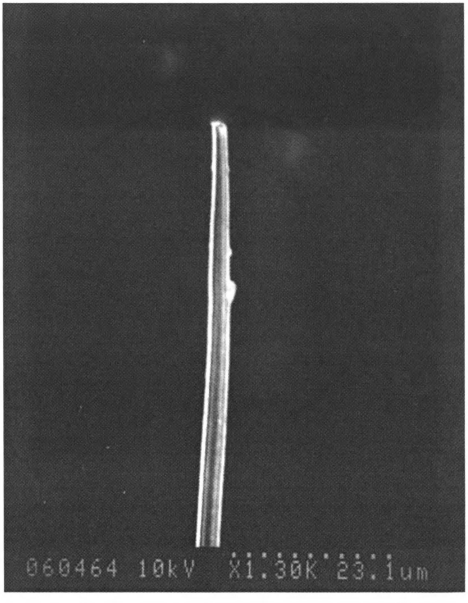

Figure 4.8 SEM image of gold probe pulled using Sutter P2000 micropipette puller.

of roughly 3-4 microns. Figure 4.9, on the other hand, clearly shows more tapering at the tip of the probe. From the scale on the micrograph, it is estimated that the tip of this

Figure 4.9 SEM image of gold and borosilicate probe.

particular probe has a diameter of approximately 500 nm. It is not clear in this image, however, if the Au is exposed at the tip. The bottom half of the probe, the brighter portion of the image, is borosilicate glass. Some results clearly show that the glass was

removed from the tip during the hydrofluoric etches. Figure 4.10 is an instance where the acid etch was not even needed. The gold wire protruded from the glass as a result of the pull. The diameter of the tip of this probe was approximately 450 nm. These images represent the best of the micro probes fabricated with the micropipette puller.

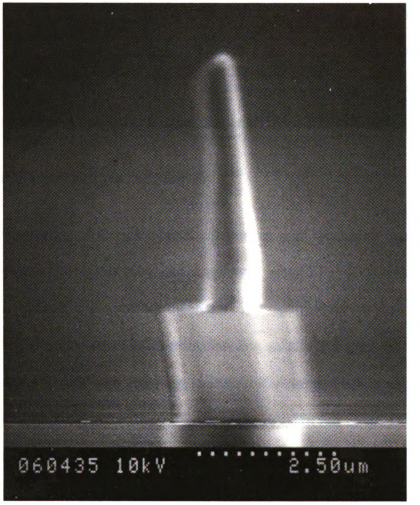

Figure 4.10 SEM image of gold micro probe.

It is quite interesting to see in this image that the final fracture of the glass is flat, although it tapered quite extensively. This type of fracture is advantageous because no hydrofluoric etch is required.

4.2 Analysis of Probe Fabrication

The elastic modulus can be calculated for the composites experimented with and compared to composites used in the literature that produced successful results. However, the elastic modulus doesn't reveal much information about the thermomechanical properties of the composite. Therefore, the viscosity of the borosilicate-gold composite will be investigated to examine how certain parameters will affect the viscosity of the composite during the pull. A low viscosity is desired, as a lower viscosity during the pull will mean the composite will flow with greater ease.

4.2.1 Calculations of Modulus of Elasticity

The elastic properties of the glass-metal composites is of interest in determining what the dimensions of the glass tube and metal wire should be to optimize the pull to achieve a sharp taper and small tip diameter. The calculations are made for the stage when the glass is pulled down to the wire diameter, as seen in Figure 4.1. Comparisons of the dimensions used and resulting modulus of elasticity values of the *Nanonics* probes [9] will be compared to the modulus of elasticity values of the probes fabricated in this research effort.

First, the elasticity for the borosilicate glass and platinum wire composite described in Fish et al. [9] will be calculated. The dimensions for the components after the glass capillary has been pulled down around the metal wire are as follows:

- Borosilicate – 0.32 mm outer diameter and 0.08 mm inner diameter
- Platinum – 0.08 mm diameter

- Platinum – 0.08 mm diameter

The modulus of elasticity for the borosilicate and platinum are 64 GPa and 171 GPa respectively. The modulus of elasticity for the composite is then (Eq. 2.7)

$$E_c = \frac{[(64.0GPa \cdot 9.6 \cdot 10^{-8} m) + (171.0GPa \cdot 6.4 \cdot 10^{-9} m)]}{1.024 \cdot 10^{-7} m} \Rightarrow$$

$$E_c = 60.0 \text{ GPa} + 10.687 \text{ GPa} = 70.687 \text{ GPa}$$

For the platinum and quartz composite designed for this research, the dimensions are:

- Silica – 0.267 mm outer diameter, 0.08 mm inner diameter
- Platinum – 0.08 mm diameter

The modulus of elasticity for the silica and platinum are 72.9 GPa and 171 GPa respectively. These values can be put into the equation to determine the modulus of elasticity for the composite.

$$E_c = \frac{[(72.9GPa \cdot 6.488 \cdot 10^{-8} m) + (171.0GPa \cdot 6.4 \cdot 10^{-9} m)]}{7.128 \cdot 10^{-8} m} \Rightarrow$$

$$E_c = 66.354 \text{ GPa} + 15.352 \text{ GPa} = 81.706 \text{ GPa}$$

For the gold and borosilicate composite designed for this research, the dimensions are:

- Borosilicate – 0.1 mm outer diameter, 0.05 mm inner diameter
- Gold – 0.05 mm diameter

The modulus of elasticity for gold is 77.2 GPa. These values can similarly be calculated using the Rule of Mixtures to find the overall modulus of elasticity for the composite.

$$E_c = \frac{[(64.0GPa \cdot 7.5 \cdot 10^{-9} m) + (77.2GPa \cdot 2.5 \cdot 10^{-9} m)]}{1.0 \cdot 10^{-8} m} \Rightarrow$$

$$E_c = 48.0 \text{ GPa} + 19.3 \text{ GPa} = 67.3 \text{ GPa}$$

These are the values for the modulus of elasticity for the three glass-metal composites analyzed.

4.2.2 Viscosity

The viscosity can be calculated for a glass-metal composite using Eq. (2.10). If the viscosity can be determined, it could help in predicting what values of parameters to input to obtain optimal results. Theoretically, the lower the viscosity for the composite, the better it should flow and the better the taper should be. Certain parameters can be varied, while the others are held constant, to see how each parameter affects the viscosity of the pipette pull.

To calculate the viscosity for the composite, the applied stress, the original length, the strain rate is needed. The initial length of the pulled down portion of the glass and metal is measured after the first pulling step, and the change in length is measured after the final pull. Also, the P-2000 displays how long it took to execute the pulls; therefore the strain rate can be calculated. The diameter of the glass and metal is known after the glass is collapsed down around the metal wire, and the force is known from the PULL parameter. Thus, the viscosity for each pull can be calculated from Eq. (2.10). Table 4. 1 lists several values of viscosity where the HEAT value on the micropipette puller is varied while the other parameters are held constant.

Figure 4.11 is a plot of these data points and it can be clearly seen that HEAT values between 365 and 375 result in the lowest viscosity for the composite. The other parameters were

- Filament – 4

- Delay – 0
- Pull – 70

This is nearly the same program that was used to fabricate the probes of Figures 4.8 – 4.10.

Table 4.1 Table of values where viscosity is calculated for different HEAT values. Each of the other parameters was held constant.

HEAT	ΔL (mm)	Time (sec)	$\Delta L/\Delta t$ (mm/sec)	Viscosity (Pas)
315	0.00943	1.82	0.00518	6.29E+09
335	0.00863	1.41	0.00612	5.33E+09
355	0.00817	1.18	0.00692	4.71E+09
365	0.01358	1.12	0.01213	2.69E+09
375	0.0138	1.14	0.01211	2.69E+09
395	0.00846	1.04	0.00813	4.01E+09

Viscosity was determined for pulls where the VELOCITY parameter was increased as the other parameters where held constant. The VELOCITY parameter dictates at what level of glass viscosity should the hard pull initiate. Table 4.2 presents the calculated viscosity that is a result of changing VELOCITY values.

The lowest viscosity value was obtained at a VELOCITY value of 40. The other parameters were set to:

- Heat – 365
- Filament – 4
- Delay – 0
- Pull – 70

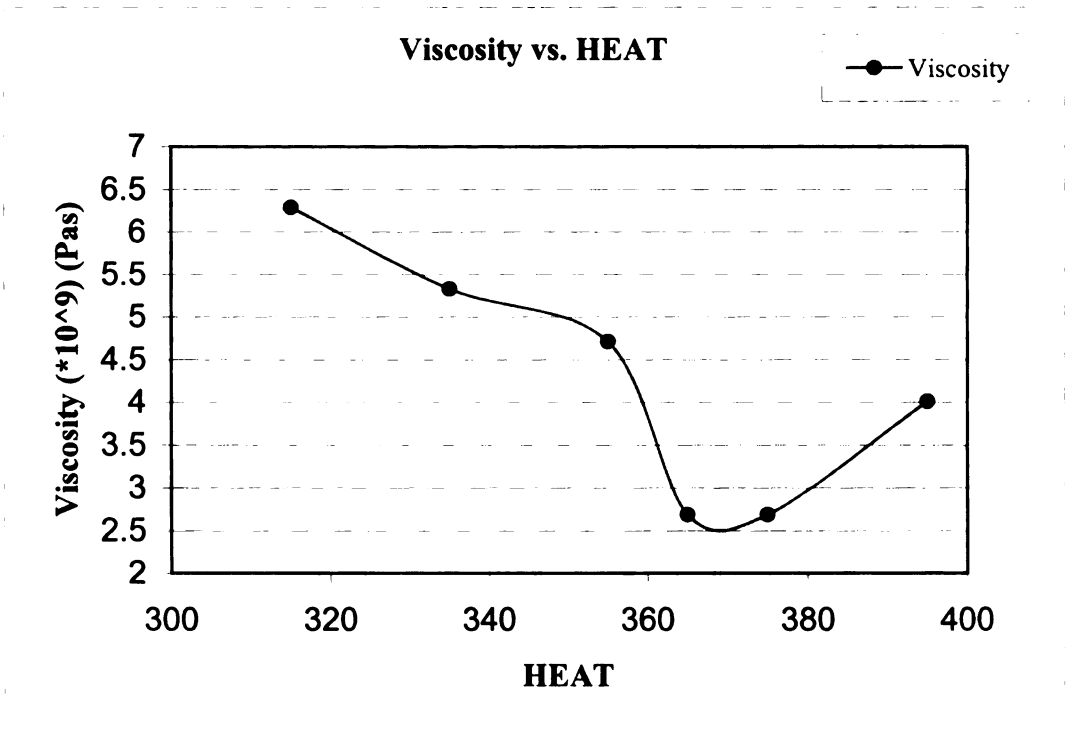

Figure 4.11 Plot of the data in Table 4.1. Values of HEAT between 365 and 375 result in the lowest viscosity of the composite.

Table 4.2 Values of viscosity for different values of VELOCITY.

VELOCITY	ΔL (mm)	Time (sec.)	$\Delta L/\Delta t$ (mm/sec)	Viscosity (Pas)
20	0.01028	1.31	0.00785	4.15E+09
40	0.014	1.21	0.01157	2.82E+09
60	0.0081	1.28	0.00633	5.15E+09
80	0.01017	1.36	0.00748	4.36E+09
100	0.01035	1.23	0.00841	3.87E+09

Figure 4.17 shows the trend of this data, where it can be seen that a VELOCITY value of 40 results in the lowest viscosity and, consequently, the best pulling result.

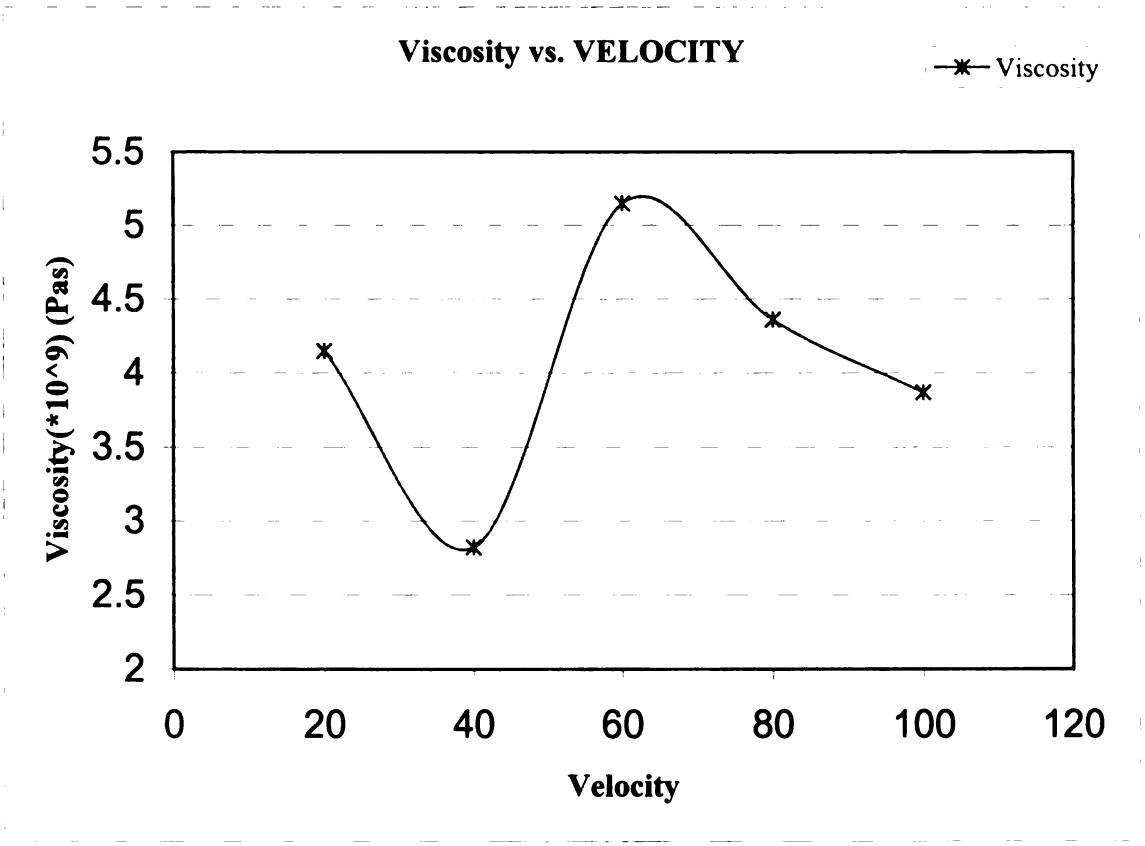

Figure 4.12 Plot of viscosity versus VELOCITY for Au/Borosilicate microprobe fabrication.

4.3 Conductivity Measurements

Conductivity measurements on different samples were carried out using the probes fabricated with the micropipette puller. The probe was mounted on a *xyz* translation stage and was used as one of the voltage probes. A sample of bismuth telluride (Be_2Te_3), a thermoelectric material, was scanned across its surface to obtain the results of its electrical conductivity. This sample was measured using a platinum/silica

microprobe as seen in Figures 4.3 and 4.4. The results of the measurement will yield the contact resistance and the electrical conductivity of the sample.

4.3.1 The One-Point Scanning Probe Method

The one-point scanning probe configuration is depicted in Fig 4.13. This illustration how the micropipette-based probe was integrated into the altered four-point probe set up as a scanning probe. The micro probe was mounted on a *xyz* translation stage so that the conductivity could be scanned across the surface of the material being tested. Contacts were made on the sample by electrochemical deposition of nickel on the sides. The current was supplied through these contacts and the low voltage was measured at that point as well. The scanning probe was used as the high voltage probe.

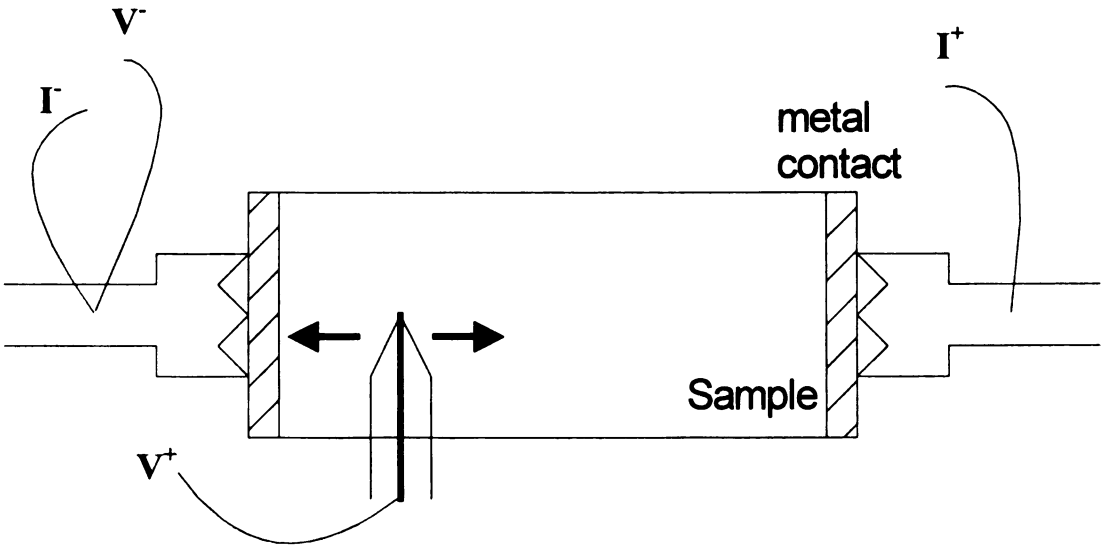

Figure 4.13 Scanning one-point probe configuration for conductivity measurement on a given sample.

An advantage of the method used, consider it a one-point scanning probe, is that the probe spacing is not held constant. This allows for the conductivity measurement of the sample along with the measurement of the contact resistance between the sample and the deposited metal electrodes.

Therefore, the scanning one-point method is simply a variation on the four-point probe technique, which allows for the measurement of the contact resistance by measuring the voltage drop at the contact.

4.3.2 Electrical Conductivity Measurements Using Pt Microprobes

Platinum micro probes were integrated into the one-point scanning probe configuration (Fig 4.13). Figure 4.14 is a plot of voltage difference versus change in probe spacing measured on a sample of bismuth telluride (Bi_2Te_3), a thermoelectric material. The measurement was done using one of the Pt electrodes similar to the one seen in Figure 4.4 to demonstrate the effectiveness of the probes. The value for the conductivity for the sample can be extracted from this data using the formula

$$\sigma = \frac{I\Delta l}{\Delta V A}, \qquad (4.2)$$

where I is the applied current, Δl is the distance between the probes, ΔV is the measured voltage difference, and A is the cross-sectional area of the sample. Below (Table 4.3) is data obtained from an AC measurement on Bi_2Te_3 using a Pt microelectrode. The contacts were made by electro deposition of nickel.

A lock-in amplifier was used to supply the oscillating sinusoidal signal with a 1 Ω resistor connected in parallel to the sample

Table 4.3 Collection of electrical conductivity data of Bi_2Te_3 using the scanning probe conductivity technique [10].

Probe Spacing (cm)	ΔV (mV)
0	0.05
0.025	0.051
0.05	0.052
0.075	0.055
0.1	0.057
0.125	0.059
0.15	0.061
0.175	0.063
0.2	0.064
0.225	0.065
0.25	0.069
0.265	0.071
0.3	0.075
0.325	0.075
0.35	0.079
0.375	0.082
0.4	0.084
0.425	0.086
0.45	0.099

This data is plotted in Figure 4.14. A large jump in voltage difference is seen between the last two data points. The contact resistance between the nickel-plated contact and the sample can be identified as it accounts for the large jump in ΔV, from 0.086 mV to 0.099 mV, when all previous values for ΔV were approximately 4 mV. Thus, simply taking the difference between these last two data points and dividing it by the applied current can determine the contact resistance for this situation.

$$R_{contact} = \frac{0.099(mV) - 0.086(mV)}{9.76(mA)} = 1.33m\Omega$$

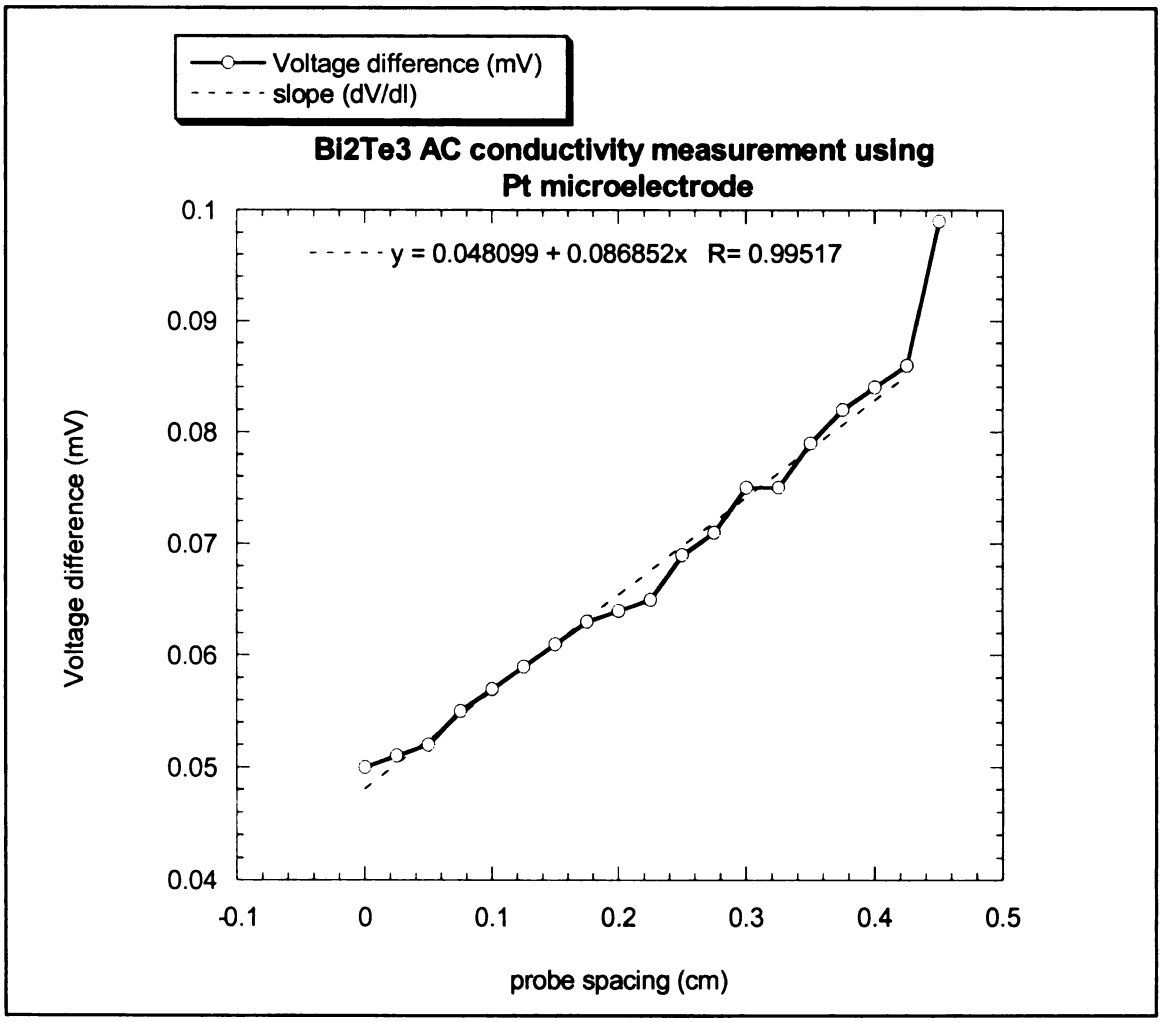

Figure 4.14 Plot of AC conductivity measurement on Bi_2Te_3 sample using Pt micro probe [10].

The slope of the plot in Figure 4.14 represents the change in voltage difference over the change in probe spacing and Eq. (4.2) can be written as

$$\sigma = \frac{I}{\left(\frac{\Delta V}{\Delta l}\right) \cdot A}, \tag{4.3}$$

by dividing the top and bottom by Δl. The current used for this conductivity measurement was 9.76 mA and the cross-sectional area of the sample was 0.103 cm^2.

Therefore, the electrical conductivity can be obtained by placing these values into Eq. (4.3).

$$\sigma = \frac{9.76(mA)}{0.08968(mV/cm)\cdot 0.103(cm^2)} = 1058.72(S/cm)$$

The accepted value for the conductivity for Bi_2Te_3 lies between 800 and 1200 *S*/cm [10].

5. CONCLUSION

5.1 Submicron Scanning Probe Measurement System

Submicron probes were created from glass capillary tubes and gold and platinum metal wires using a CO_2 laser-based micropipette puller. Probes with tip diameters of less than 500 nm were fabricated using methods developed during this research, and integrated into a scanning one-probe measurement system. This system features the ability to measure the electrical conductance of a sample along with the contact resistance between the sample and the current lead. Another feature of the system is the potential to measure low-scale dimension samples. The probe system was successfully tested on a 0.231 cm^2 Bi_2Te_3 sample using a Silica/Pt probe as the scanning probe. However, with probe tips less than 500 nm, much smaller samples could be measured.

The viscosity of the glass-metal composite can be determined for any of the settings of the P2000. This property was investigated, and for the borosilicate-gold probes, the program developed for the fabrication yielded the lowest viscosity, and consequently the most uniform tapers and smallest tip diameters.

5.2 Suggestion for Future Work

5.2.1 Mount Probes in Microprobe Station

The measurements done for this research were carried out under a low magnification optical microscope and a simple translational stage. This led to several broken probes, as they are fragile and deform under relatively small levels of pressure. Our research group recently acquired a microprobe station similar to the one depicted in

Figure 1.2. The station features digital micrometers for translation of the probe, a vibration-free working surface, a high magnification optical microscope, a turbomolecular vacuum pump, and a temperature controller.

The submicron probes could be mounted into this probing station and be used as a scanning electrode, similar to the configuration used in this research, with much better manipulation control and visual capability. Much of the glass would have to be etched away to mount the probes into the station, however. The probes are fed through a small hole and clamped into place with a setscrew. This setscrew is also an electrical contact for the probe. If the probe is covered in glass, it will be electrically insulated from the rest of the system and there will also be difficulty clamping it into position. Therefore, the glass should be etched away approximately 1 cm up the probe length. This will allow for contact with the bare wire both electrically and mechanically.

5.2.2 Continued Improvement on Probe Fabrication Procedure

Further research should be built on the research that has been accomplished on the fabrication of submicron probes. Supplementary research into gold and platinum probes will eventually lead to smaller and smaller probe tips, ideally down to 50 nm. The programs designed for the micropipette puller can be further manipulated in attempt to achieve smaller probe tips. Another area of interest lies in developing programs that will pull silica glass and gold wire together. There is interest in growing silicon nanowires by pulsed laser deposition on the tips of metal-filled micropipettes. This would yield a nanowire that is wieldable and is grown directly onto an electrical contact, as depicted in Figure 6.1.

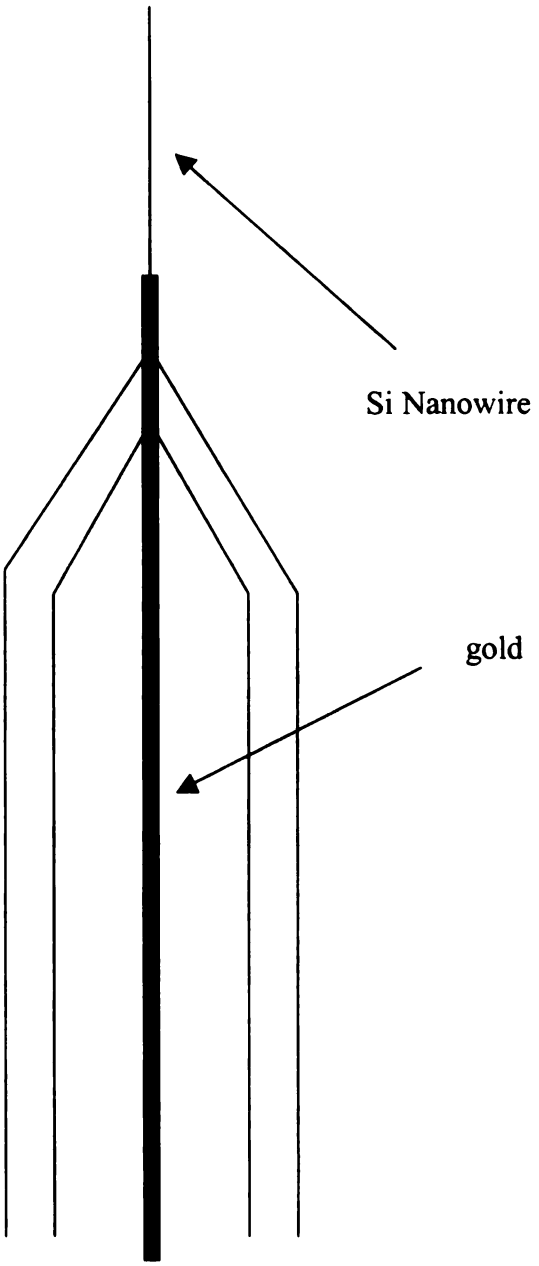

Figure 5.1 Illustration of Si nanowire grown off tip of silica-gold submicron electrode.

APPENDIX A

Below are tables of temperature dependant properties of platinum and platinum alloys.

Table A.1 Temperature dependant properties of pure Pt [20].

Temp. (°C)	Elastic Modulus (GPa)	Mod. Of Rigidity (GPa)	Poisson's Ratio
25	164.6	54.2	0.518
200	159.3	52.9	0.506
400	153.3	51.1	0.5
500	149.1	50	0.491
600	145.6	48.9	0.489
700	141.9	47.7	0.487
800	137.8	46.6	0.479
900	132.7		

Table A.2 Temperature dependant properties of Pt 10%Rh [20].

Temp. (°C)	Elastic Modulus (GPa)	Mod. Of Rigidity (GPa)	Poisson's Ratio
25	212.6	78	0.363
200	206.3	75.4	0.368
400	197.9	72.1	0.372
500	193.3	70.5	0.371
600	188.7	68.7	0.373
700	183.9	66.9	0.374
800	179.2	65.2	0.38
900	175	63.4	
1000	169.7		
1100	164.9		

Table A.3 Temperature dependant properties of Pt 10%Ir [20].

Temp. (°C)	Elastic Modulus (GPa)	Mod. Of Rigidity (GPa)	Poisson's Ratio
25	202.3	73.4	0.378
200	196.6	71.1	0.382
400	188.3	68.1	0.382
500	183.9	66.4	0.385
600	178.8	64.8	0.381
700	173.6	62.8	0.381
800	170.7	58.1	
900	166.4		
1000	162.2		
1100	157.1		
1200	150.8		

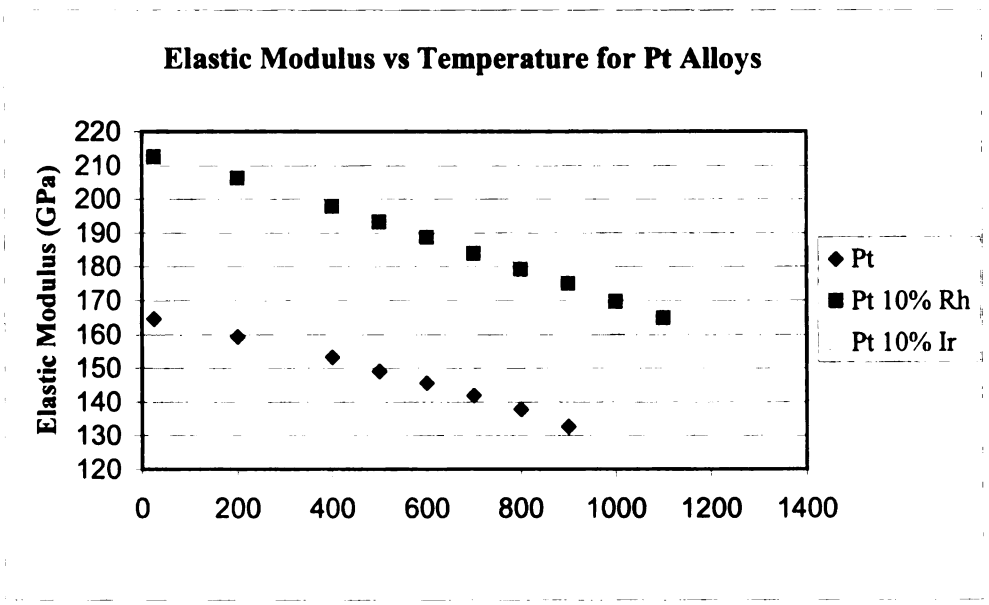

Figure A.1 Comparison of elastic modulus vs. temperature between pure Pt, Pt 10%Rh, and Pt 10%Ir [20].

7. REFERENCES

1. Robert M. Dowben and Jerzy E. Rose, "A Metal-Filled Microelectrode", *Science*, Vol. 118, pp. 22-24,1953.

2. Bradford D. Pendley and Hector D. Abruna, "Construction of Submicrometer Voltammetric Electrodes", *Analytical Chemistry*, Vol. 62, No. 7, pp. 782-784, 1990.

3. **www.nanonics.co.il**

4. G. Tallarida, "Imaging P-N Junctions by Scanning Near Field Optical Microscopy, Atomic Force and Electrical Contrast Microscopy", *Materiali e Dispositivi per la Microelettronica,* pp. 1-2.

5. D.J. McComas and G.P. Miller, "Space applications of microelectromechanical systems: Southwest Research Institute® vacuum microprobe facility and initial vacuum test results", *Review of Scientific Instruments*, Vol. 74, No. 8, pp 3874-3878, May 2003.

6. **www.janis.com**

7. Lei Huang, Wanjun Wang, and Michael C. Murphy, "Peltier-effect module for highly localized temperature manipulations", *Review of Scientific Instruments*, Vol. 70, No. 11, pp. 4398-4403, August 1999.

8. Mun-Heon Hong, Ki Hyun Kim, "Scanning nanolithography using a material filled nanopipette", *Applied Physics Letters*, Vol. 77, No. 16, p. 2605, 2000.

9. G. Fish, O. Bouevich, S. Kokotov, K. Lieberman, D. Palanker, I. Turovets, and Aaron Lewis, "Ultrafast response micropipette-based submicrometer thermocouple", *Review of Scientific Instruments*, Vol. 66, No. 5, pp. 3300-3306, May 1995.

10. A. Kubota, "Scanning Probe Electrical Conductivity Measurements Using Submicro-Electrodes Fabricated by Nonlithographic Methods", Masters Thesis, Michigan State University, 2003.

11. Callister, William D., Materials Science and Engineering: An Introduction, 4th Edition, New York, John Wiley & Sons, 1997.

12. Gibson, Ronald F, Principles of Composite Material Mechanics, McGraw-Hill Inc., 1994

13. Z. Li, J. Lambros, "Dynamic thermomechanical behavior of fiber reinforced composites", *Composites Part A*, Vol. 31, pp 537-547, 2000.

14. Savitsky E.M., The Influence of Temperature on the Mechanical Properties of Metal and Alloys, Stanford University Press, 1957.

15. Groover, Mikell P., Fundamentals of Modern Manufacturing, Prentice Hall, Inc., 1996.

16. G. Banuprakash, V. Katyal V.S.R. Murthy, and G.S. Murty, "Mechanical behaviour of borosilicate glass-copper composites", *Composites Part A*, Vol. 28A, pp. 861-867, May 1997.

17. Robert H. Doremus, "Viscosity of silica", *Journal of Applied Physics*, Vol. 92, No. 12, pp. 7619-7629, August 2002.

18. **www.matls.com**

19. R. L. Williamson, B.H. Rabin, and J.T. Drake, "Finite element analysis of thermal residual stresses at graded ceramic-metal interfaces. Part I. Model description and geometrical effects", *Journal of Applied Physics*, Vol. 74, No. 2, pp 1310-1320, July 1993.

20. Jurgen Merker and David Lupton, "High Temperature Mechanical Properties of the Platinum Group Metals", *Platinum Metals Rev.*, Vol. 45, No. 2, pp. 74-82, 2001.

21. G.M. Bartenev, The Structure and Properties of Inorganic Glasses, Wolters-Noordhoff Publishing, 1970.

22. Narottam P. Bansal and R.H. Doremus, Handbook of glass properties, Orlando: Academic Press, 1986.

23. **www.sutter.com**

24. Sutter Instrument Company, P-2000 micropipette puller operation manual.